Histol Histopathol (1997) 12: 1091-1124

Histology and Histopathology

Invited Review

Techniques and application of microscopic radioautography

T. Nagata
Department of Anatomy and Cell Biology, Shinshu University School of Medicine, Matsumoto, Japan

Summary. The techniques for light and electron microscopic radioautography developed in our laboratory are described. The outlines of the applications to various tissues and organs are also briefly summarized.

First, the techniques are explained in detail. These techniques can be divided into two categories, i.e., chemical fixation followed by wet-mounting radioautography and cryo-fixation followed by dry-mounting radioautography. The former is limited in application to only insoluble compounds, while the latter is universally applicable to any kind of compounds including soluble compounds. Both procedures, the chemical fixation wet-mounting procedure and the cryo-fixation dry-mounting procedure at light and electron microscopic levels are described.

Next, the applications of both the procedures to various compounds are briefly mentioned. Chemical fixation with glutaraldehyde and osmium tetroxide followed by wet-mounting radioautography demonstrates insoluble macromolecular synthesis such as nucleic acids (both DNA and RNA), proteins, glucides and lipids. On the other hand, cyro-fixation followed by dry-mounting radioautography demonstrates soluble small molecular compounds such as macromolecular precursors, hormones, neurotransmitters, vitamins, inorganic compounds and drugs or toxins.

These procedures are expected to be applied for various inorganic and organic compounds in living organisms to elucidate the sites of their incorporation, synthesis and discharge.

Key words: Light microscopy, Electron microscopy, Radioautography, Technique, Application, Organ system

Offprint requests to: Dr. Tetsuji Nagata, Department of Anatomy and Cell Biology, Shinshu University School of Medicine, Matsumoto 390, Japan

1. Introduction

In order to estimate cellular functions of various organs, tissues and cells of animals, various methodologies are now available in life sciences including morphological, physiological and biochemical procedures. Among them, one of the methods to demonstrate sites of incorporation, syntheses and discharge of various substances in living organisms by means of light and electron microscopic radioautography to localize intracellular sites of metabolism at cellular and organelle levels, has been developed in our laboratory during these 40 years. We have developed simple routine standard techniques to demonstrate insoluble compounds in various cells and tissues of experimental animals and to quantitate the contents of synthesized macromolecules in each cell and cell organelle by both light and electron microscopy. The localization of silver grains developed by means of ordinary radioautography, however, demonstrates only the insoluble radioactive substances bound to the macromolecules fixed in the cell with the chemical fixatives used (Nagata, 1992). On the other hand, radioisotopes bound to the small molecules which are not fixed with ordinary chemical fixatives are washed away through conventional routine procedures such as fixation, dehydration, embedding, sectioning, and radioautographic procedures, so that these compounds cannot be demonstrated. Ordinary radioautographic procedures can be designated as wet-mounting radioautography, since the tissues are processed through both conventional wet treatments and applying wet radioautographic emulsions to the specimens. In order to demonstrate any soluble radioactive compounds, special techniques are required in accordance with the characteristics of the radioisotopes used for radioautography. The techniques of radioautography of soluble compounds can be theoretically classified into two categories from the viewpoint of fixation used as shown in Table 1 (Nagata et al., 1969, 1977b). In the precipitation method, the labeled soluble compound is fixed in a mixture containing a substance which reacts with the soluble radioactive compounds forming a

Table 1. Principles of techniques for microscopic radioautography demonstrating soluble and insoluble compounds.

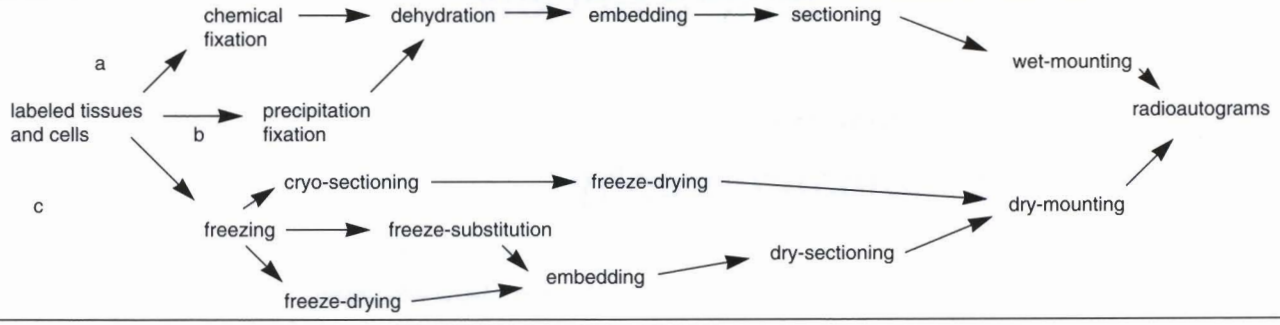

a: radioautography for conventional insoluble compounds; b: precipitation procedure of radioautography for soluble compounds; c: freezing procedure of radioautography for soluble compounds.

precipitation, so that the fixed tissues can be processed through routine histological procedures followed by a routine wet-mounting radioautography to demonstrate the labeled precipitation. This principle was first used in detecting soluble ^{45}Ca by Nagata and Shimamura (1958, 1959a,b) in light microscopic radioautography of several tissues fixed in a formaldehyde solution containing ammonium oxalate to form calcium oxalate precipitation. At the electron microscopic level, Mizuhira et al. (1968) later used this method for fixing the tissues labeled with ^{3}H-thiamine with a glutaraldehyde solution containing platinum chloride to form thiamine-PtCl6 precipitation, or fixing labeled ^{3}H-cholesterol with a mixture containing digitonin. This procedure, however, is limited to the radioactive compounds which can be precipitated with any other specific compounds. Moreover, there are many possibilities of diffusion of the labeled compounds when they are precipitated with the fixatives.

By the freezing method, on the other hand, the labeled tissues are quickly frozen in a cooled liquid such as isopentane or propane cooled to its melting point with liquid nitrogen. Then the tissues can be cut by cryomicrotomy. At light microscopic level, the frozen tissues can be cut in a cryostat at a thickness around 20-30 μm and the frozen sections are placed in contact with radioautographic emulsions by various techniques. Many papers have been published on this problem. We first used a large-wire loop to produce dry films which were air-dried and applied to cryostat sections placed on glass slides (Nagata and Nawa, 1966). This procedure is very convenient and will be described in detail. At the electron microscopic level, however, only a few papers have been published on this principle; cyro-ultramicrotomy. Appleton (1964) and Christensen (1971) discussed the possibility of this method but they did not show the results, while we (Nagata and Murata, 1977) reported the results for the first time. On the contrary, Mizuhira et al. (1981) and Futaesaku and Mizuhira (1986) reported a new technique for ultramicrotomy utilizing interposed films, which is however not an ideal procedure because it employs cryosectioning after tissues have been immersed into sucrose solution and picking up cryosections with sucrose droplets and touching them with wet radioautographic emulsion.

On the other hand, freeze-dried or freeze substituted tissues can be embedded in paraffin or resin for light microscopy and dry sections mounted on precoated slides. Edwards and Udupa (1957) and Smitherman et al. (1963) used freeze-dried and paraffin embedded sections. Miller et al. (1964) applied the wire-loop method as part of the dry mounting procedure at light microscopic level. We improved this technique first at light microscopic level (Nagata and Nawa, 1966) and then applied it at electron microscopic level (Nagata and Murata, 1977). Stirling and Kinter (1967) embedded freeze-dried tissues in silicon-araldite and the plastic sections were wet-mounted with a dropping procedure but not dry-mounted.

This paper deals with the techniques of light and electron microscopic radioautography which were developed in our laboratory and the results applied to histology and histopathology of respective organ systems in animals and man.

2. Principles of radioautography

Radioautography is the technique used to make the specimens come into contact with photographic emulsions and give exposure for a certain period of time to produce the latent images of the radioactive substances in the specimens, then to develoop the emulsion to produce the silver metal grains, thus enabling the researchers to compare both the specimens and radioautograms in order to find the localization of radioactive substances in the specimens. For these procedures, 3 fields of knowledge, physics concerning the radioactivity, histology dealing with the fixation, embedding, sectioning and staining tissues and cells, and photographic chemistry treating photographic emulsions, are needed.

Table 2. Classification of radioautography.

SOLUBILITY OF COMPOUNDS	SIZE OF SPECIMENS			
	Macro-radioautography		Micro-radioautography	
	whole-body	organ	LM	EM
Insoluble RAG	insoluble whole-body RAG	insoluble organ RAG	insoluble LMRAG	insoluble EMRAG
Soluble RAG	soluble whole body RAG	soluble organ RAG	soluble LMRAG	soluble EMRAG

Table 3. Radio-isotopes used in microscopic radioautography.

NUCLIDE	HAL-LIFE	RAYS EMITTED	PARTICLE ENERGY (KeV)
^{3}H	12.5 years	beta	18.5
^{14}C	5760 years	beta	155
^{32}P	14.2 days	beta	1710
^{35}S	87 days	beta	167
^{45}Ca	165 days	beta	250
^{56}Fe	3 years	Auger electron	14
^{125}I	60 days	Auger electron	35
^{203}Hg	45 days	beta	208

Table 4. Radio-labeled compounds used in microscopic radioautography.

RESEARCH PURPOSE		RADIO-LABELED COMPOUNDS
Macromolecular precursors		
Nucleic acids,	DNA	^{3}H-thymidine
	RNA	^{3}H-uridine
Proteins,	secretory granules	^{3}H-glycine, ^{3}H-leucine, etc
	collagen	^{3}H-proline, ^{3}H-hydroxyproline
Glucides,	simple polysaccharides	^{3}H-glucose, ^{3}H-glucosamine, etc
	mucosubstances	$^{35}SO_4$
Lipids		^{3}H-glicerol, ^{3}H-fatty acids, etc
Target tracers (small molecular compounds)		
Hormones		^{3}H-steroids, ^{3}H-insulin, etc
Neurotransmitters		^{3}H-GABA, ^{3}H-dopamine, etc
Vitamins		^{3}H-vitamin A, B, C, D, etc
Inorganic substances		$^{22}NaCl$, $^{45}CaCl_2$, $^{203}HgCl_2$, etc
Drugs		^{3}H-antibiotics, ^{3}H-anti-allergics, etc
Toxins and others		^{3}H-ouabain, ^{3}H-strychnine, etc

2.1. Classification of radioautography

Since the experimentally-produced radioautograms include varieties of specimens, i. e. human biopsy material, experimental animal tissues and cells or even whole bodies of small animals, the size of the specimens varies according to the samples. Larger specimens such as whole bodies or large organs are designated as macro-radioautograms which are observed with the naked eye. On the contrary, small samples such as small pieces of tissues or cells are observed with microscopes; either light microscopes or electron microscopes. This is called as microscopic radioautography. Macroscopic radioautography can be classified into two levels, whole body radioautography and organ radioautography, while microscopic radioautography can be classified into light microscopic radioautography and electron microscopic radioautography. On the other hand, they are also divided into two categories; soluble compound radioautography and insoluble compound radioautography from the view point of solubility of the radioactive compounds (Nagata, 1992). The classification of these two combinations are listed in Table 2.

2.2. Radioactive compounds

The radioactive compounds used in radioautography are mainly composed of inorganic or organic compounds which are artificially labeled with radio-isotopes (RI) and can be incorporated into human or animal bodies by experiments. The radioactivity emitted from the radioactive compounds is divided into 3 kinds, i.e. alpha, beta and gamma rays. The alpha ray is the helium nucleus in nature and has low energy, weak penetrability, strongest ionization and shortest range (μm), the beta ray is the electron and has medium energy, medium penetrabilty, medium ionization and shorter range (μm-mm), while the gamma ray is the electro-magnetic wave and has high energy, strong penetrability, low ioniazation and the longest range (m). Among these 3 rays, the beta ray is the best for radioautography because of its shorter range and the strongest ionization. For radioautography various kinds of RIs are used, which are listed in Table 3. Among them, ^{3}H, ^{14}C, ^{35}S and ^{125}I are very often utilized for both macro- and micro-radioautography because they can be labeled to various inorganic compounds which are usually used in biological and medical researches. Since the radioactivity of respective RI decreases time-dependently but never reachs zero, the life of an RI is defined as half-life; the time required for the RI to lose 50% of its initial radioactivity. The half lives of ^{3}H or ^{14}C are longer (years) than ^{35}S or ^{125}I (days) as listed in Table 3, so that the experiments using shorter half-life compounds should be completed within a shorter period.

In histology and histopathology, the RI-labeled compounds used for radioautography can be classified into 2 categories, i.e. the precursors which are incorporated into macromolecules such as nucleic acids (DNA and RNA), proteins, glucides and lipids, and the other target tracers which are small molecular compounds such as hormones, neurotransmitters, vitamins, inorganic substances, drugs and others (Table 4). All the RIs should be treated only in the RI

laboratories according to the regulations concerning radiation damage in respective countries.

2.2. Administration of radioactive compounds

The radioactive compounds labeled with specific RIs are usually administered orally to small animals such as rats and mice or by injections given subcutaneously, intramuscularly, intravenously and intraperitoneally. For the purpose of demonstrating macromolecular synthesis, animals were injected intraperitoneally with radioactive precursors for macromolecular syntheses at varying concentrations at 1-50 μCi (37-1850 kBq)/gram body weight for macro-RAG and for LMRAG or 10-100 μCi (370-3700 kBq)/g.b.w. depending on the characteristics of the compounds and RIs used. The RI-labeled precursors used in our experiments were ^{3}H-4-thymidine (Amersham, England, specific activity 877 GBq/mM) for DNA synthesis, ^{3}H-uridine (Amersham, England, 1.11 TBq/mM) for RNA, ^{3}H-4,5-leucine (Amersham, 1.04 TBq/mM) and ^{3}H-taurine (New England Nuclear, USA, specific activity 74 GBq/mM) for proteins, ^{3}H-1-glucosamine (Amersham, 105 GBq/mM) for polysaccharides, ^{35}S-sulfuric acid (Amersham, 1.11 TBq/mM) for mucosubstances and ^{3}H-1,2,3-glycerol (Amersham, 7.4 GBq/mM) for lipids.

Sometimes in vitro labeling can be carried out in cultured cells, both established cell lines or primary culture and tissue blocks obtained from human biopsy or necropsy materials, in media containing radioactive compounds at concentrations of 1-100 μCi (37-3700 kBq) per ml medium, using CO_2 incubator under normal conditions at 37 °C with 5% CO_2 in air or pathological conditions, for varying time intervals from several minutes up to several hours.

2.3. Animal treatment and tissue processing

After administrations of radioactive compounds by either oral administration or injections, all the small animals such as mice and rats are anesthetized by intraperitoneal injections with pentobarbital sodium (Nembutal, Abbott Laboratories, Chicago, Ill., USA), and sacrificed at a given time, usually 1 hour after the RI administration, either by decapitation or by perfusing via the left ventricles of the hearts with 2.5% glutaraldehyde in 0.1M cacodylate buffer at pH 7.2 depending on whether insoluble or soluble radioautography will be carried out. For conventional insoluble radioautography perfusion fixation can be used and the tissues from various organs taken out, cut into small pieces (1x1x1 mm), soaked in the same glutaraldehyde fixative at 4 °C for 1 hour and postfixed in 1% osmium tetroxide in the same buffer for 1 hour, dehydrated with graded ethanol and embedded in epoxy resin (Epon 812 or Epok 812, Oken Co., Tokyo, Japan). On the other hand, in vitro labeling of cultured cells and tissue blocks obtained from either animals or human biopsy materials are incubated in media containing radioactive compounds, using CO_2 incubator under normal conditions at 37 °C for a given time, usually 1 hour or up to a few hours. They are then rinsed in Hanks' solution, fixed in the same buffered glutaraldehyde and osmium tetroxide solutions, dehydrated and embedded in epoxy resin as above.

For the soluble radioautography, however, perfusion fixation cannot be used. The whole bodies of the small animals or organs and tissues taken out after decapitation without using any solution, should be immediately cryofixed by either metal contact method or immersion method (Nagata 1994a), and be processed by cryosectioning or freeze-drying or freeze-substitution.

Embedded tissues in epoxy resin can be used for either LMRAG or EMRAG. For LMRAG, thick sections at 2 μm are cut on an ultramicrotome and picked up onto clean glass slides and warmed for extension and drying. For electron microscopy, ultrathin sections of 100 nm thickness are cut in general using a conventional transmission electron microscope with the accelerating voltage at 100 kV. It is generally accepted that the thinner the section the better the resolution, but the less radioactivity it contains the longer the exposure time for radioautography. If any intermediate high voltage electron microscope is available such as accelerating voltages of 200, 300 or 400 kV, thicker sections, at 200 or 300 nm thick, can be used. We prefer to use semithin sections at 200 nm thickness at 400kV in order to shorten the exposure time. Semithin sections are cut on a Porter-Blum MT-2B ultramicrotome (Dupont-Sorvall, Newtown, CONN, USA). Ultramicrotomes of mechanical feeding type are preferable than thermal feeding type because of the accuracy of the section thickness, which effects the number of silver grains by radioautography. Ultrathin or semithin sections are picked up onto either platinum or gold meshes in order to prevent the copper meshes from rusting through the histological and radioautographic treatment, especially by development. Alternatively, collodion coated copper grid meshes can be used. For collodion coating, copper grid meshes (100-200 meshes) are soaked in 2% collodion solution for a few min, spread on filter paper in a Petri dish and dried at 37 °C for a few hours in an incubator.

2.4. Photochemistry

The photographic emulsion in general consists of both matrix of gelatin and photosensitive silver halide crystals which are embedded in gelatin. The nuclear emulsions used for radioautography are sensitive for radiation and consist of gelatin matrix and silver bromide crystals. The silver bromide crystals produced by several photo-industry makers are uniform in size ranging from 70 to 400 nm in diameter depending on their brands. Several kinds of emulsions are commercially available in several countires. They are classified into four types, i.e., gel form or bulk liquid emulsions for light and electron microscopy, stripping

films for LMRAG, coated plates or films for macro-RAG and LMRAG, and coated films for macro-RAG. We prefer to use bulk liquid emulsions produced by Konica Co. Tokyo, Japan, Konica NR-M2 for LMRAG and Konica NR-H2 for EMRAG, because of their fine grains and high sensitivity. Other types of emulsions such as Kodak NTB2, 3, 5, or Ilford K-2 and L-4 can also alternatively be used.

There are various techniques published for applying radioautographic emulsions to the specimens, depending on the kinds of specimens and radioactive compounds to examine. The procedures should be described in detail according the methodologies employed in the following sections. After the specimens make contact with the emulsions, they are kept in a cold (4 °C) dark room, usually in a light tight slide box kept in a refrigerator, for exposure for several weeks and developed. The development is a chemical reaction to reduce the silver bromide crystals and to convert them to metallic silver grains. When the emulsion is soaked in a developer, the developer reduces the silver bromide crystals which contain specks of latent images building more and more metallic silver around the latent image. The size of silver grains depends on the constituents of the developer, the time and temperature of development. The standard developers such as Kodak D-19 or Konica SD-X1 consist of some reducing reagents such as methol and hydroquinone, which are abbreviated as MQ developers. When MQ developers are used for both LM and EMRAG, large spiral silver grains as long as a few μm are grown, which are too large for electron microscopy. On the contrary, when fine grain developer such as gold latensification and phenidon developer at a low temperature and shorter time is used, small dot-like silver grains less than 1 μm in diameter are produced, which are preferable for electron microscopy (Nagata, 1992).

3. Techniques of microscopic radioautography

The techniques for microscopic radioautography developed in our laboratory can be divided into 2 categories, wet-mounting radioautography for insoluble compounds such as macromolecular synthesis and dry-mounting radioautography for soluble compounds such as small molecular compounds. Each can be sub-divided into 2 methods, respectively, light microscopy and electron microscopy (Table 1).

3.1. Chemical fixation wet-mounting radioautography

3.1.1. Preparation of tissues

Small animals such as mice and rats are anesthetized and sacrificed either by decapitation or by perfusing via the left ventricles of the hearts with 2.5% glutaraldehyde in 0.lM cacodylate buffer at pH 7.2 and the tissues from various organs are taken out, cut into small pieces, soaked in the same glutaraldehyde fixative at 4 °C for 1 hour and postfixed in 1% osmium tetroxide in the same buffer for 1 hour, dehydrated with graded ethanol and embedded in epoxy resin. On the other hand, cultured cells and tissue blocks, incubated in media containing radioactive compounds in vitro, using CO incubator under normal conditions at 37 °C for a given time, are rinsed in Hanks' solution, fixed in the same buffered glutaraldehyde and osmium tetroxide solutions, dehydrated and embedded in epoxy resin as above. The tissue blocks are cut on an ultratome for either LM (2 μm thick) or EM (0.1-2 μm) and picked up onto either glass slides or grid meshes using water.

3.1.2. Light microscopic wet-mounting radioautography

For light microscopic wet-mounting radioautography, the same tissue blocks for electron microscopy, which were fixed in buffered glutaraldehyde and osmium tetroxide solutions then embedded in epoxy resin, are cut on a Porter-Blum MT-2B ultramicrotome at 2 μm thickness (semithin sections) and are mounted on microscopic glass slides. In order to produce many radioautograms at once and also to compare each other quantitatively, the following procedures, which were developed in our laboratory (Nagata, 1982, 1992; Nagata et al., 1961, 1967a), are carried out.

1) A bottle of bulk emulsion (we use Konica NR-M2 emulsion, Konica Ltd., Tokyo, Japan), is melted in a water bath at 45 °C for about 10 minutes, to which an equal amount of distilled water is added (Fig. 1A) and mixed for 5-10 min with a glass slide to remove all air bubbles. Then, a slide holder, made of stainless steal, holding 15 glass slides which carry several semithin sections, is dipped into the melted emulsion for several seconds, then they are pulled up vertically for about 3 seconds to assure equal thickness coating (3-4 μm) over the sections (Fig. 1B). The faster the speed is, the thinner becomes the emulsion coating.

2) The bottom of the slide holder is wiped with a paper towel to remove excess emulsion (Fig. 1C) and the slide holder is placed in an electric incubator at 28 °C with a humidity of about 80%, containing a wet sponge at the bottom, and dried for 1 hour. When the slides are dry, they are stored in a light tight slide box containing a desiccant (silica gel). After the edge of the box is sealed with black tape, it is kept in a refrigerator at 4 °C for exposure (Fig. 1D).

3) After an appropriate exposure time, all the slides are developed at once by pouring the developer into the slide box (Fig. 1E). We use Konica KD-X1 (formerly SD-X1) developer for Konica NR-M2 emulsion. Kodak D-19 may be used for any type of emulsions. After the development, the slides are rinsed in stop bath (2% aqueous acetic acid solution), fixed in a fixer (30% aqueous sodium thiosulphate solution) for 5 minutes twice, washed gently in running tap water for 10 minutes, and finally they are stained in 1% toluidine blue solution for light microscopy.

3.1.3. Electron microscopic wet-mounting radioautography

Tissues embedded in epoxy resin can be used for either LMRAG or EMRAG. For LMRAG, thick sections at 2 μm are cut on an ultramicrotome and picked up onto clean glass slides and warmed for extension and drying. For EMRAG, ultrathin sections at 0.1 μm (100nm) or semithin sections at 0.2 μm (200nm) can be cut on an ultramicrotome and picked up on collodion-coated grid meshes. The semithin sections should be observed by high voltage electron microscopy (Nagata, 1995b).

As for the radioautographic emulsions, several types of emulsions are commercially available. We use Konica NR-H2 emulsion (Konica Ltd., Tokyo, Japan) because of the small sized silver bromide crystals and better sensitivity. To obtain thin monolayers of silver bromide crystals, two techniques, dipping and wire-loop methods, are now in general use. The choice lies between mounting the sections on a flat microscopic glass slide or on a grid mesh during the exposure. By the former method, glass slides are covered with thin collodion films on which sections are placed and they are coated with radioautographic emulsion by dipping similarly to the light microscopic procedure. After exposure and photographic processing, the sections and collodion films together with the emulsion are floated off the glass slide and picked up on a grid for examining by electron microscopy. This procedure is called a flat substrate method and is, in practice, very complicated and troublesome. On the other hand, by the latter method, sections are placed on grid meshes coated with collodion films according to the normal sectioning method and are covered with a preformed monolayer emulsion by picking up thin bubbles of molten emulsion on a wire-loop and allowing it to gel before touching it on the grids. This is called the wire-loop method. We prefer this procedure, which was developed at our laboratory, using either small wire-loops (Fig. 3A) or larger wire-loops (Fig 2B), and it appears rather easier. Our procedure is described in detail as follows (Nagata, 1992, 1996a; Yoshida et al., 1978).

1) A regular square glass block, whose side length is 1. 25 cm, is made from glass strips No. 4890-40 for LKB knife maker (LKB-Produkter AB, Bromma, Sweden). A square piece of double-coated Scotch tape, 4 mm in length, is stuck on the surface of each glass block. Six grids are placed around the tape like a rosette, arranged clockwise to identify each grid (Fig. 2A). The grids are vacuum coated with carbon at 10 nm thickness.

2) Radioautographic emulsion is diluted in equal parts with distilled water at 45 °C. We use Konica NR-

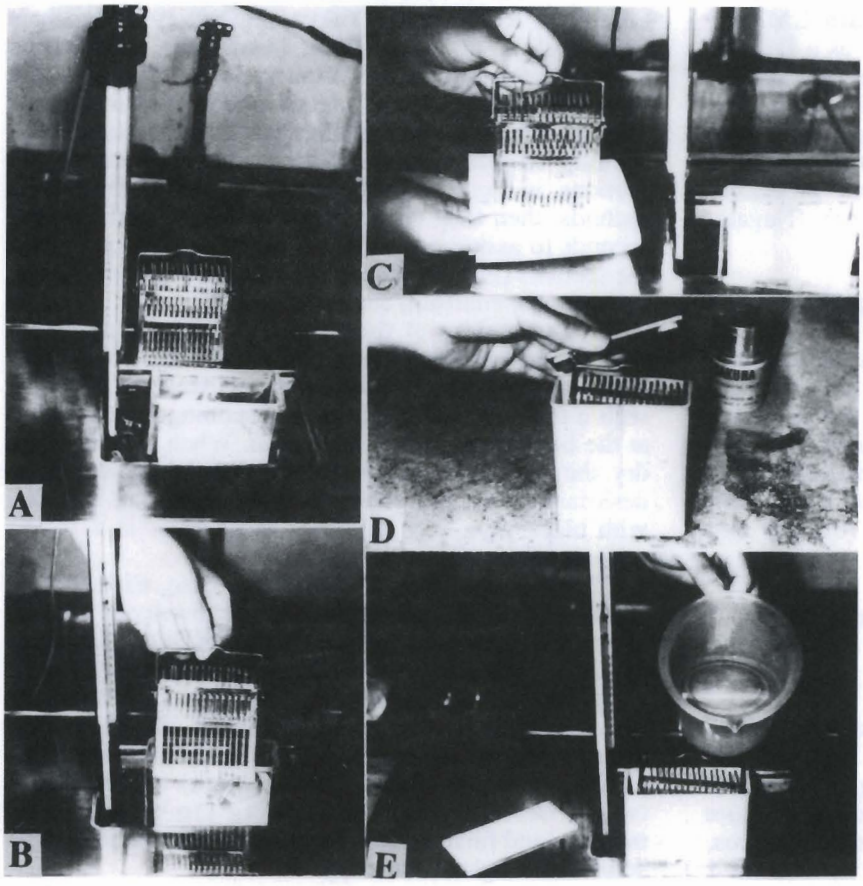

Fig.1. The standard procedure for preparing light microscopic radioautograms by wet-mounting radioautography. **A.** Bulk emulsion is melted by diluting with distilled water at 45 °C in a staining jar. **B.** A slide holder holding 15 slides is dipped into melted emulsion and pulled up vertically. **C.** Excess emulsion is wiped off with tissue papers. **D.** After the slides are dried, the slide holder is stored in a light tight slide box for exposure. **E.** After appropriate exposure, the developer is poured into the slide box and the slides are developed at once.

H2 emulsion from Konica (formerly Sakura) Ltd., Tokyo, Japan. Any other emulsions such as Kodak can alternatively be used. Ten ml of diluted emulsion is added with 0.2 ml at 2% aqueous solution of dioctyl sodium sulfosuccinate (a surfactant) in order to prevent the emulsion film from bursting (Nagata and Nawa, 1966). A thin film of emulsion is obtained by dipping a wire-loop, 2.5 cm in diameter, which is made of platinum wire or vinyl coated iron wire (Fig. 2B) in the solution.

3) After air-drying horizontally for 1 min, when the emulsion film is gelled but still wet, the film is applied horizontally to the grids on the glass block (Fig. 2C). The glass block is warmed at 28 °C for 1 hour for in order to dry the emulsion.

4) For exposure, several glass blocks are attached to one side of a microscopic slide with double-coated Scotch tape (Fig. 2D)

5) Control emulsion films should be checked by electron microscopy before the exposure (Fig. 2E)

6) Several glass slides, carrying several glass blocks, respectively, are placed in a black light tight plastic slide box which contains desiccant (silica gel), and the top is sealed with black tape (Fig. 2F). The slide box is kept in a refrigerator at 4 °C for exposure.

7) After an appropriate exposure time, the glass slides carrying glass blocks with grid meshes are processed for development (Fig. 2G), then stopped in a stop bath, fixed in a fixer and stained with lead citrate solution for electron staining.

As for the development of the emulsions, when a conventional MQ-developer such as D-19 is used, long spiral silver grains are formed (Fig. 10). In order to obtain smaller silver grains, phenidon developer after gold latensification (G-L) is recommended (Figs. 5, 6, 11, 12, 14). We prefer the following procedure (Murata et al., 1979; Nagata, 1992).

1) The glass slides which carry grid meshes are first soaked in distilled water in a staining jar for 10 seconds.

2) They are then soaked in G-L solution (2% aqueous gold chloride solution 0.2 ml, potassium thiocyanate 0.05 g, potassium bromide 0.06 g, distilled water 100

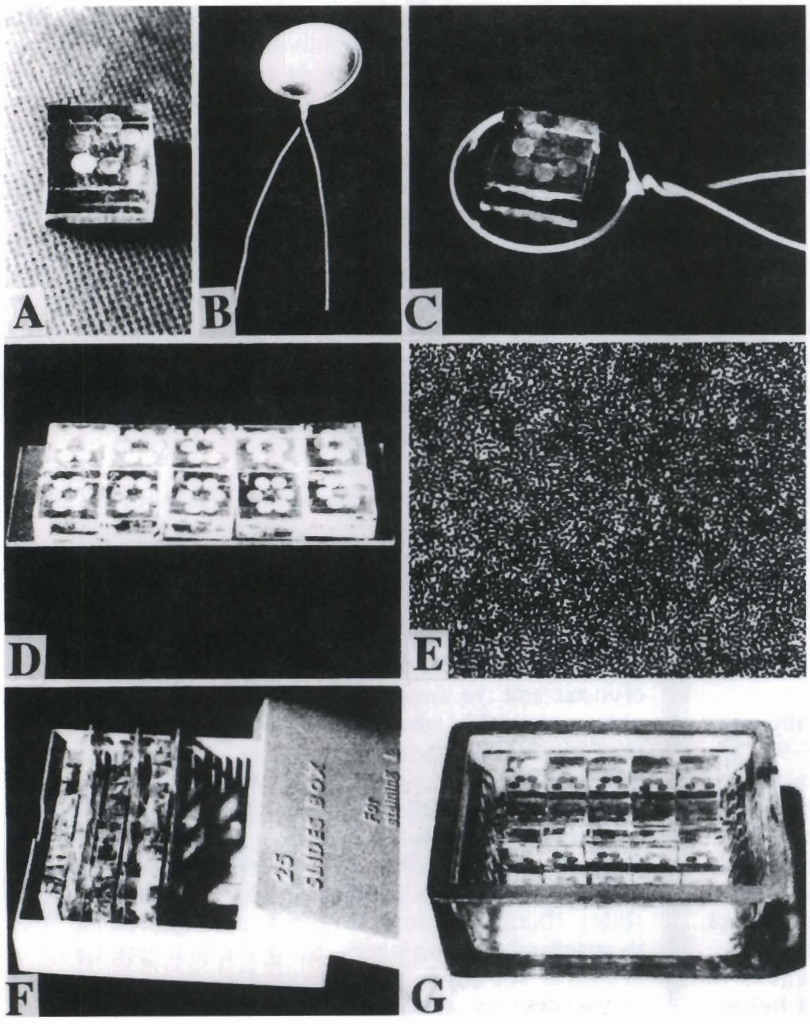

Fig. 2. The standard procedure for preparing electron microscopic radioautograms by wet-mounting radioautography. **A.** Six meshes which carry several sections respectively are placed on a square glass block. **B.** A wire-loop is dipped into melted emulsion and a thin film of emulsion is obtained. **C.** When the emulsion film gelled, it is applied horizontally to the meshes on the glass block. **D.** Ten glass blocks carrying 6 meshes respectively are attached onto a glass slide with Scotch tape. **E.** Transmission electron micrograph of monolayer silver bromide crystals in Konica NR-H2 emulsion film before development. **F.** Several glass slides, each carrying 10 glass blocks, are stored in a slide box for exposure. **G.** After exposure, all the meshes on glass blocks are developed at once, then fixed and stained.

ml) for latensification at 16 °C for 30 seconds.

3) The slides are then rinsed in distilled water for 10 seconds.

4) They are soaked in phenidon developer (ascorbic acid 1.5 g, phenidon 0.25 g, potassium bromide 0.4 g, potassium carbonate 1.3 g, sodium sulfite anhydrous 20 g, potassium thiocyanate 4.0 g, distilled water 100 ml) in a water bath at 16 °C for 60 seconds for development.

5) They are soaked in a stopper solution (2% aqueous acetic acid solution) for 10 seconds.

6) They are fixed in a fixer (30% aqueous sodium thiosulphate solution) for 5 minutes, 2 changes.

7) They are rinsed in distilled water for 5 minutes, 3 changes.

8) The sections are stained in lead citrate solution (Reynolds, 1963) for 3 minutes.

9) They are rinsed in distilled water for a few minutes.

10) Finally the grids are carefully removed from the glass blocks with forceps and placed on a filter paper in a Petri dish and dried in an incubator at 37 °C for 1 hour.

11) The specimens are coated with carbon in a vacuum coater at about 10 nm thick before electron microscopy.

3.2. Cryo-fixation dry-mounting radioautography for soluble compounds

To demonstrate soluble small molecular compounds, cryo-fixation and dry-mounting radioautography should be employed for both LMRAG and EMRAG.

3.2.1. Preparation of tissue blocks.

After the tissues are taken out without using any solution from the experimental animals which had received injection of radioactive compounds, they are trimmed as small as 1x0.5x0.5 mm with two pieces of razor blades on a cold plate cooled to 0 °C with ice and water. The tissue blocks are attached to small pieces of aluminum foil, 5x5 mm in size (Nagata, 1994a) or onto the surface of a metal block. Cultured cells are centrifuged at 500 rpm for 10 minutes after incubation in the media containing radioactive compounds, and the pellet is placed on a piece of aluminum foil.

3.2.2. Freezing procedure

The quenching fluids used are propane (melting point -169 °C), isopentane (-161 °C), or hexane (-94 °C). These reagents are liquids at low temperatures and conduct heat very well. They also bubble when they contact tissues. Among them, propane is explosive, while hexane has a rather higher melting point. Therefore, isopentane is very often used (Nagata, 1994a). Instead of quenching fluids, a pure copper block is sometimes used in direct contact with the tissues.

As cooling agents, the following substances or mixtures of two substances are used: liquid helium (boiling point -269 °C); liquid nitrogen (-196°C); liquid air (-190 °C); dry ice and ether (-60°C); or dry ice and nonane (-53 °C). Among these, liquid nitrogen is most frequently used. We usually use the combination of isopentane or propane as the quenching fluid and liquid nitrogen as the cooling agent, or a copper block as metal contact and liquid nitrogen as the cooling agent. Recently, cryoinstruments such as RF-2 (Eiko, Tokyo, Japan), JFD-RFA (JEOL,Tokyo, Japan), cryoblock or cryovacublock (Reichert-Jung, Germany) are commercially available.

Liquid nitrogen (200-300 ml) is carefully poured into a Dewer flask. A 50 ml beaker is placed in the liquid nitrogen, and 20-30 ml of isopentane or propane is poured into the beaker. The authors prefer isopentane to propane. Within a few minutes the liquid isopentane begins to solidify at its melting point of -160 °C as it is cooled by the liquid nitrogen at -196 °C. The tissue blocks or free cells adhering to a small piece of aluminum foil are plunged quickly into the isopentane with a pair of forceps. The aluminum foil should be released from the forceps quickly rather than putting the forceps into the isopentane. If the forceps are put into the isopentane, the aluminum foil will adhere to them. The frozen tissues are then removed from the isopentane, using a small cup, which is made with a piece of aluminum foil 3 cm x 3 cm in size, moulded with a No. 00 gelatin capsule in order to prevent ice crystal formation, and transferred into liquid nitrogen in a Dewer flask, and stored under the liquid nitrogen until processing. In this process, if the tissues are exposed to the air, ice crystals will grow larger, and the fine structure will be damaged. The frozen tissues are then processed through freeze-drying or freeze-substitution procedures. In case of metal contact method, using cryoinstruments, frozen tissues are removed from the copper blocks and stored in the liquid nitrogen as well.

3.2.3. Cryo-sectioning

The frozen tissues can directly be cut by cryo-sectioning without any embedding. The procedures for cryo-sectioning can be divided into two, light microscopic and electron microscopic cryo-sectioning.

3.2.3.1. Light microscopic cryo-sectioning. At light microscopic level, the frozen tissues can be cut in a cryostat and the frozen sections placed in contact with radioautographic emulsions. Kinter et al. (1960) placed sections directly on the photographic plates and clamped them for exposure. Fitzgerald (1961) applied dry films on sections mounted on slides. Appleton (1964) placed sections on precoated slides at a low temperature. Stumpf and Roth (1964, 1966, 1969) transferred freeze-dried sections onto either siliconized slides or Teflon slides. Hammarstrom et al. (1965) used cellophane tapes to attach sections on plates. Since the first application of cryostat sections on precoated slides at very low temperature by Appleton (1964), many authors such as

Rogers et al. (1965) have used this technique at light microscopic level.

The frozen tissues can be sectioned directly without embedding by means of cryo-sectioning. For light microscopy we use a conventional rotary type cryostat. The frozen tissues are transferred into a cryostat kept at around -30 °C and dry sections at 20-30 μm are cut. They are transferred onto glass slides and either air-dried at room temperature or freeze-dried at -30 °C for a few hours. The latter procedure is better than the former. When cryostat sections picked up onto precoated slides and air-dried at room temperature, the sections melt and cause diffusion of soluble compounds. This procedure is called thaw-mount radioautography and can be applicable when the diffusion is negligible.

3.2.3.2. Electron microscopic cryo-sectioning. The technique of ultrathin cryo-sectioning, or simply cryo-ultramicrotomy, was first reported by Bernhard and Leduc (1967). Then, it was improved by Tokuyasu (1973), employing preincubation in sucrose solution and picking up sections with sucrose droplets. For radioautography, however, his technique is not applicable because of the diffusion. We use LKB ultratomes 4800 equipped with an LKB cryokit 14800 or LKB-NOVA (LKB, Bromma, Sweden). Other types of ultramicrotomes such as DuPont-Sorvall or Reichert-Jung with cryokits can be used. The temperature of the specimen is usually set at -100 °C to -120 °C and that of the glass knife at -80 °C to -100 °C. The optimal temperature depends on the kind of tissues used. Dry sections are picked up with dry eyelash probes onto grids and covered with another grid like a sandwich and pressed with copper rods according to Christensen (1971) or Sakai et al. (1974). The authors use a modified apparatus of Sakai type. Grids used for this purpose are coated with collodion applied by soaking copper grids in 1% collodion solution and dried at 37 °C for 1 hour. As controls, wet sections are picked up with sucrose droplets (Nagata et al., 1978a). Grids carrying dry sections are dried through freeze-drying at -50 °C for 24 hours, like the freeze-drying procedure of tissue blocks as described above. Among the drying procedures tested, i. e. freeze-drying, freeze-substitution, and air-drying, the freeze-drying procedure is the best from the viewpoint of preservation of both cell structure and radioisotopes (Nagata, 1994a). In order to freeze-dry cryosections, we use a rotary cryotransfer apparatus modified after Sakai et al. (1974). The rotary disc, which carries 5 grids with cryosections, is changed every 5 grids and transferred into a carrier, which consists of a tube and a cylinder which can contain 5 discs in its shelves, thus containing 25 grids (Nagata, 1994a). The carrier is transferred into the desiccator of the freeze-drying apparatus, which is operated for 3 hours at -80 °C. After the cryosections are dried, they are coated with carbon and are processed through the dry-mounting radioautographic procedure. Recently, cryotransfer apparatuses are commercially available affiliated to respective cryo-kit equipped ultramicrotomes such as LKB, Sorvall or Reichert.

3.2.4. Freeze-drying procedure

The freeze-drying technique was first used by Altmann (1890), then was applied for light and electron microscopy by Gersh (1932, 1956). The freeze-drying apparatus we are using was designed and constructed by the present author (Nagata et al., 1969; Nagata, 1994a) in our laboratory. It consists of a cold trap, a desiccator, which is set in the cold trap, three Geisler, discharge and ionization vacuum gauges, and two rotary and oil diffusion vacuum pumps. The cold trap consists of a stainless steel cylinder containing liquid nitrogen. The desiccator, which is set in the cold trap, has 96 sets of thermoelements which can be controlled with electric current at temperatures between -80 °C to +60 °C. The whole apparatus is capable of maintaining a pressure of less than 10^{-6} Torr. A similar apparatus is now commercially available from several makers. The frozen tissues are ladled into the freeze-drying apparatus with a small aluminum cup. The freeze-drying should be carried out at first with the operation of the rotary pump for about an hour until the pressure reaches 10^{-3} Torr. The two pumps (RP and DP) are then operated for about 24 hours to complete drying, while the desiccator is kept at -80 °C. After the completion of freeze-drying, the temperature is maintained over several hours by changing the electric current of thermoelement, so that the whole drying procedure takes about 30 hours. Before completion of the procedure, the epoxy embedding mixture is placed in the dripping unit which should be evacuated for 10 minutes by means of another rotary pump at a pressure of 10^{-3} Torr. After completion of drying, the embedding medium (epoxy resin mixture) is dripped down into the specimen chamber, the tissues are infiltrated and the two pumps are stopped. When the drying procedure is completed, the tissues adhering to aluminum foil will sink in the embedding medium. Fixation is not required before the embedding, although Pearse (1968) maintains that the unfixed freeze-dried tissues are easily damaged. In this case, when fixation is preferable before embedding, in order to enhance contrast, freeze-dried tissues can be exposed to osmium vapor for 30 minutes in a tight jar containing a small piece of osmium tetroxide crystal. Freeze-dried tissues are taken out and infiltrated with fresh embedding medium overnight at room temperature, and polymerized at 35 °C, 45 °C and 60 °C for 12 hours each according to Luft (1961). When cultured cells on grids are freeze-dried, no embedding is necessary. The freeze-dried grids are processed through radioautography directly and can be observed by high voltage electron microscopy (Nagata et al., 1977b; Nagata, 1995b).

3.2.5. Freeze-substitution

The technique of freeze-substitution or freeze-thawing was applied to light microscopy by Simpson

(1941) for the first time and was developed later by Lison (1960). At electron microscopic level, several papers describing the morphology of freeze-substituted cells have been published (van Harrevelt and Crowell, 1964; Trump 1969). The principle of freeze-substitution is to dehydrate the frozen tissues in a solvent at a very low temperature without thawing the tissues, and substitute the ice with the solvent. The usual solvents are acetone, ethanol or ether. The coolants used are dry ice-acetone mixture (-78 °C) or dry ice-ethanol (-78 °C). We applied this principle to radioautography for the first time (Nagata, 1972). The procedure is as follows:

1) Dry ice and acetone are mixed in a Dewer flask.

2) A small test tube or sample tube containing 20-30 ml of absolute acetone is put in the Dewer flask and cooled to -78 °C.

3) Tissues are frozen according to the procedure described above in liquid nitrogen, and transferred with aluminum foil cups into the test tube containing absolute acetone.

4) The transferred tissues are kept in the substituting fluid for 72 hours to substitute the ice with the solvent. The present authors use a deep freezer (Tabai, Tokyo, Japan) in which the Dewer flask is stored and the temperature is kept at -80 °C.

5) After the substitution is completed, the temperature is gradually raised to 20 °C over several hours. The tissues are transferred into Epon/acetone mixture, then processed through Epon mixture and polymerized. In general, it is useful to use cryoprotective agents such as glycerine, DMSO, or sucrose in order to reduce the ice crystal formation artifacts. However, for the purpose of demonstrating soluble radioactive compounds by means of radioautography, it is preferable not to employ such techniques.

Recently, freeze-substitution instruments such as CS-auto (Reichert-Jung, Germany) which can be controlled automatically are commercially available.

3.2.6. Dry sectioning of freeze-dried or freeze-substituted material

We usually cut dry sections from epoxy resin-embedded tissues for both light and electron microscopy without using any water. By sectioning the Epon or Epok blocks of freeze-dried or freeze-substituted tissues, it is necessary to cut sections without using water in the knife trough in order to prevent diffusion artifact of labeled soluble compounds. Complete dry sectioning without any liquid is very difficult in expanding dry sections. It is also difficult to pick them up onto glass slides or grid meshes. Among many knife trough liquids which we tested, ethylene glycol was the best for flotation and expansion of the dry sections (Nagata et al., 1969). It wets the glass knife to the very edge but does not wet the plastic sections. It does not resolve soluble labeled compounds. Sections are not so easily expanded on ethylene glycol as on water, but can be expanded when they are warmed with a tungsten lamp for a few minutes. They are picked up onto collodion coated glass slides or 150 mesh grids. We use glass slides or grids which are previously coated with collodion by dipping them into 1% collodion solution and drying them at 37 °C for 1 hour.

3.2.7. Dry-mounting procedure

Both cryo-sectioned and freeze-dried specimens and freeze-dried or freeze-substituted and embedded specimens should be coated with dry radioautographic emulsions without using any water. The procedure is designated as dry-mounting radioautography. The procedures for dry-mounting radioautography can be divided into two, light microscopic and electron microscopic procedures.

3.2.7.1. Light microscopic dry-mounting procedure. Historically various procedures were employed in the literature for light microscopic dry-mounting radioautography. For example, Kinter et al. (1960) placed sections directly on the photographic plates and clamped them for exposure. Fitzgerald (1961) applied dry films on sections mounted on glass slides. Appleton (1964) placed sections on precoated slides by dipping at a low temperature. Stumpf and Roth (1964, 1966, 1969) transferred freeze-dried sections on either siliconized slides or Teflon slides. Hammerstrom et al. (1965) used cellophane tapes to attach sections on plates. Since the first application of cryostat sections on precoated slides at very low temperature by Appleton (1964), many authors have recommended this technique at light microscopic level. However, those procedures are very complicated for the treatment of both specimens and emulsions. We first used dry-films produced with a large wire-loop which was air-dried and applied to cryostat sections placed on glass slides (Nagata and Nawa, 1966). We believed that this method is the most convenient one. The procedure is as follows.

1) Cyrostat sections are picked up onto glass slides and dried. Dry epoxy resin sections are expanded over the slides with a drop of ethylene glycol without using any water.

2) Radioautographic emulsion is diluted in equal parts with distilled water at 45 °C. We use Konica NR-M2 emulsion from Konica (formerly Sakura) Ltd., Tokyo, Japan. Any other emulsions such as Kodak can alternatively be used. Ten ml of diluted emulsion is added with 0.2 ml at 2% aqueous solution of dioctyl sodium sulfosuccinate (a surfactant) in order to prevent the emulsion film from bursting (Nagata and Nawa, 1966).

3) A thin film of emulsion is obtained by dipping a wire-loop, 2.5 cm in diameter, which is made of platinum wire or vinyl coated iron wire and set with a piece of Scotch tape on a glass slide as a handle (Fig. 3A).

4) The handle is set horizontally on a flat desk for air-dring.

5) After air-drying for 1-2 min, when the center of the emulsion film is gelled and dried appearing transparent but the peripheral zone is still wet, appearing opaque, the film is applied to the slide horizontally (Fig. 3B).

6) The glass slide is kept in a Petri dish and warmed at 28 °C in an incubator for 1 hour to dry the emulsion.

7) Several glass slides are placed in a black light tight plastic slide box which contains desiccant (silica gel), and the top is sealed with black tape. The slide box is kept in a refrigerator at 4 °C for exposure.

8) After an appropriate exposure time, the glass slides are processed for development, then stopped in a stop bath, fixed in a fixer and stained with toluidine blue solution for staining.

9) Control tissues should be fixed with chemical fixative, dehydrated, embedded, wet-sectioned and wet-mounted by conventional dipping procedure.

3.2.7.2. Electron microscopic dry-mounting procedure. After the ultrathin sections are prepared, grids are coated with emulsion. In the case of tissues fixed with precipitation fixation, on the other hand, the ultrathin Epon sectioning and radioautography can be carried out according to the routine wet-mounting procedures.

With tissues fixed by freezing, however, freeze-dried or freeze-substituted tissues are dry-sectioned and have to be radioautographed by the dry-mounting procedure (Nagata et al., 1969). The grids carrying dry sections (either freeze-dried or freeze-substituted Epon-embedded sections or freeze-sectioned and freeze-dried) are coated with carbon at 5-10 nm thick. They are put on a grid holder made of a glass slide (25 mm x 75 mm) and 3 glass rods (3 mm in diameter and 10 mm in length, respectively (Fig. 3C)).

1) Radioautographic emulsion is diluted to 1 part in 10 with distilled water at 45 °C in the dark room.

2) Ten ml of the diluted emulsion is added to 0.2 ml of 2% aqueous solution of dioctyl sodium sulfosuccinate and is maintained at 45 °C in a thermobath for several minutes to complete mixing. Dioctyl sodium sulfosuccinate, a surface activating agent is used to prevent the emulsion films from bursting while they are being dried in the air (Nagata and Nawa, 1966; Nagata et al., 1969, 1977a). The authors use Konica NR-H2 emulsion, produced by Konica Co., Ltd., Tokyo, Japan. Other emulsions for electron microscopic radioautography such as Kodak NTB or Ilford L4 can be used in a similar way. All the procedures are as follows.

3) A thin film of the emulsion thus prepared is obtained by dipping a platinum wire loop, about 1 cm in diameter (Fig. 1A), into the emulsion (Nagata et al., 1969).

4) Instead of a small platinum wire loop, a large vinyl coated iron wire loop, 2.5 cm in diameter (Fig. 2B), can also be used (Yoshida et al., 1978; Nagata, 1992).

3) The handle of the wire loop is set on a flat surface for air-drying (for 1-2 minutes).

4) The best condition for applying the film to the grid is in such a way that the peripheral zone of the film

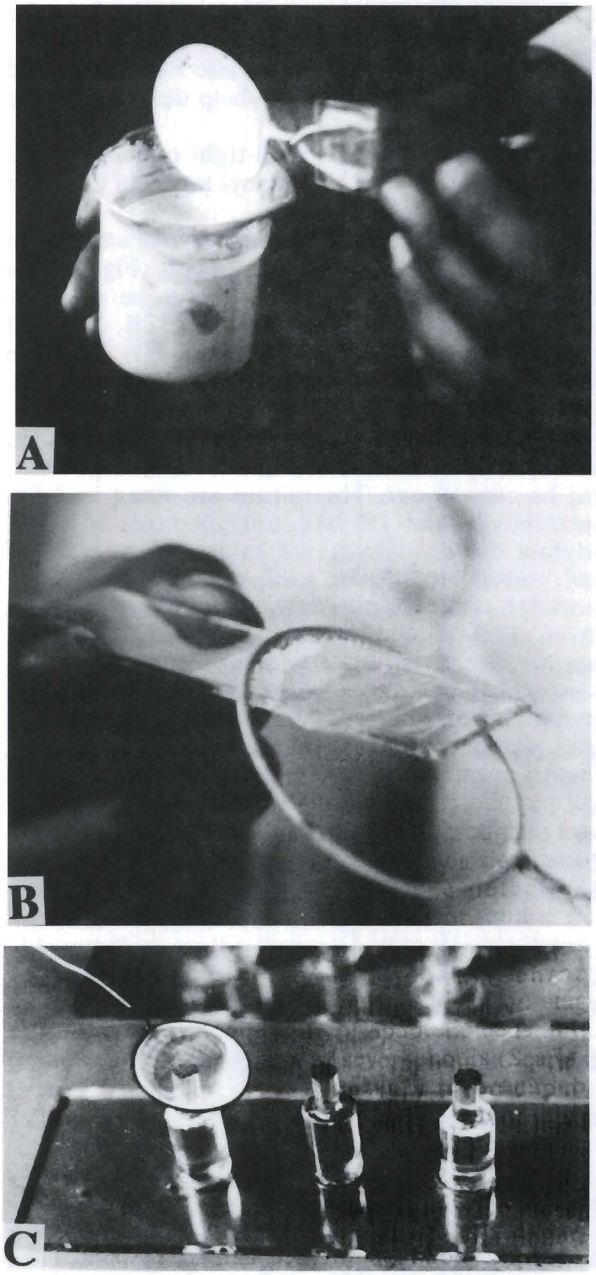

Fig. 3. The special procedures for preparing light and electron microscopic radioautograms by dry-mounting radioautography to demonstrate soluble compounds. **A.** A large wire-loop, 2.5 cm in diameter, for LMRAG is dipped into melted emulsion and a thin film of emulsion is obtained. **B.** When the emulsion film is dry, it is applied horizontally to the glass slide carrying specimens. **C.** Photograph of a small wire-loop, 1 cm in diameter, for EMRAG, showing the procedure for EM dry-mounting radioautography applying the dried film to the grid on the grid holder similarly to the game of the quoits.

appears gelled but wet (opaque) while the central zone is gelled and almost dry appearing transparent. The films are almost 100% air-dried without breaking by use of dioctyl sodium sulfosuccinate solution. Without this agent, the films will burst most of the time (Nagata and Nawa, 1966).

5) The dried films are then applied to the grids on the holders like quoits (Fig. 3C).

6) The grids are then transferred into Petri dishes and are warmed at 37 °C for 1 hour to help the films adhere to the grids.

7) The grids are kept in a light-tight container with desiccant and sealed with black vinyl tape and kept in a refrigerator at 4 °C for exposure.

On the other hand, when several grids are attached to a square glass block, 12.5 mm in length (Fig. 2A), a large wire-loop, 2.5 mm in diameter, can be similarly used to the wet-mounting procedure (Fig. 2B, 2C), and several blocks are placed on a slide (Fig. 2D). They are exposed, developed, fixed and stained simultaneously (Fig. 2F, 2G).

As the control, radioautography by means of conventional procedures for insoluble compounds, should be carried out. The tissues are fixed in 2.5% glutaraldehyde and 1% osmium tetroxide in 0.1M cacodylate buffer, dehydrated in a graded series of ethanol, embedded in Epon, sectioned with water in the knife trough, and wet-mounted with radioautographic emulsion. Following an adequate exposure time, the meshes are transferred into developer. The author uses gold-latensification and phenidon developer (Murata et al., 1979). Other types of developer such as Kodak D-19 can also be used. Following processing through stopper, fixer and several rinses of distilled water, the grids are stained in a lead citrate solution for 3 minutes for the purpose of both staining and removing the gelatin of the emulsion. We use lead citrate solution consisting of 10 ml distilled water and 30 mg lead citrate, adjusted to pH 12 with a few drops of 10N NaOH solution. The lead citrate solution according to Reynolds (1963) can also be used. Uranyl staining is usually not necessary.

4. Observation of microscopic radioautograms

4.1. Light microscopy

Light microscopic radioautograms are observed by either conventional transmission light microscopy or dark field incident light microscopy. By the former method silver grains appear dark together with the stained sections, so that the localization of silver grains is clear but sometimes confusing with densely stained structures such as secretory granules. On the other hand, by the latter method silver grains appear as bright specks over the dark sections like stars in the dark sky, so that we can recognize the silver grains but cannot observe the sections well. Either method has its advantages and disadvantages.

4.2. Electron microscopy

Electron microscopy can usually be carried out with conventional transmission electron microscopes with standard voltage around 100 kV. However, we prefer to use intermediate high voltage electron microscopes such as accelerating voltages at 200, 300 or 400 kV when available to obtain better contrast between the silver grains and the cell structures. We use either a Hitachi H-700 electron microscope at 200 kV or a JEOL JEM-4000EX electron microscope at 300 or 400 kV (Nagata, 1995b).

4.3. Image analysis of microscopic radioautographs

To analyze these radioautograms quantitatively, we can make use of various kinds of image analyzers now commercially available (Nagata, 1993a, 1995c). The number of labeled nuclei per total cell populations labeled with ^{3}H-thymidine for calculating the labeling index, or the number of silver grains per cell body or per unit area labeled with other macromolecular precursors for calculating the relative incorporation rates are measured and calculated. On the other hand, direct quantitation of silver grains on EMRAG is possible by using energy dispersive X-ray microanalyzers equipped with intermediate high voltage electron microscopes with either STEM or TEM modes (Nagata, 1991, 1993a, 1995c).

5. Applications to various compounds

5.1. Macromolecular synthesis

Macromolecular compounds such as nucleic acids (DNA and RNA), proteins, glucides and lipids which are synthesized in cells and tissues can be demonstrated by wet-mounting radioautography (Nagata, 1993b, 1994c, 1995a).

5.1.1. DNA synthesis

Nucleic acids are classified into DNA and RNA. DNA (deoxyribonucleic acid) is the main component of nucleoproteins and consists of deoxyribose, phosphate, and bases which contain A (adenine), T (thymine), G (guanine) and C (cytosine). ^{3}H-thymidine is incorporated into the bases. Light and electron microscopic radioautograms of gastrointestinal tracts of mice and rats labeled with ^{3}H-thymidine revealed the localization of silver grains over nuclei of the cells during S-phase of the cell cycle, indicating the sites of DNA synthesis in epithelial cells such as the stomach mucous neck cells and crypt cells in the small and large intestines. As the result of these studies the turnover rates of epithelial cells in the intestines were clarified. Cell kinetic studies were extensively carried out by Leblond and coworkers in the 1960's (Leblond, 1981). We have mainly studied the labeling sites and labeling as

well as cell organelle changes in respective cell components in parenchymatous digestive organs such as the liver and the pancreas and a little in esophageal and intestinal epithelial cells in the aging mice from prenatal to postnatal periods by light and electron microscopic radioautography (Nagata, 1995a).

5.1.2. RNA synthesis

RNA (ribonucleic acid) is composed of ribose, phosphate and the bases, A, U, G, and C. In order to demonstrate RNA synthesis, ^{3}H-labeled cytidine was formerly used (Nagata, 1967). However, a very little ^{3}H-cytidine could also be incorporated into DNA, so that demonstration of DNase digestion was necessary to verify RNA synthesis. On the contrary, ^{3}H-5-uridine was shown to be specifically incorporated into only RNA. Therefore, it has now come to be used for the demonstration of RNA synthesis (Nagata, 1992, 1994b, 1995a). When ^{3}H-uridine is administered to animals, or cultured cells are incubated in a medium containing ^{3}H-uridine in vitro and radioautograms are prepared, silver grains first appear over the chromatin of the nucleus and nucleolus of all the cells within several minutes, then silver grains spread over the cytoplasm within 30 minutes showing messenger RNA and ribosomal RNA. We have studied quantitative changes of RNA synthesis in the liver and pancreas of aging mice by means of light and electron microscopic radioautography after injection of ^{3}H-uridine.

5.1.3. Protein synthesis

Protein consists of polypeptides and the protein synthesis of cells and tissues can be demonstrated by light and electron microscopic radioautography after administration of RI-labeled amino acids such as ^{3}H-glycine, ^{3}H-leucine or ^{3}H-phenylalanine which are incorporated into endoplasmic reticulum, Golgi apparatus and then transferred to secretory granules or cytoplasmic ground substance and finally discharged outside the cells (Nagata, 1993b, 1995b). On the other hand, ^{3}H-proline or ^{3}H-hydroxyproline are incorporated into endoplasmic reticulum and Golgi apparatus of fibroblasts and accumulated into collagen in the extracellular matrix (Oliveira et al., 1991, 1995).

5.1.4. Glucide synthesis

Glucides are classified biochemically into monosaccharides, disaccharides and polysaccharides. Monosaccharides and disaccharides are water soluble small molecules which cannot be fixed by chemical fixation, but only by cryo-fixation for soluble compounds. Therefore, only polysaccharide synthesis is usually demonstrated by conventional light and electron microscopic radioautography with chemical fixation. Polysaccharides can be classified into simple polysaccharides and complex polysaccharides. Among complex polysaccharides, glycoproteins are composed of proteins and sugar chains, which incorporate ^{3}H-labeled glucose, galactose, fucose, N-acetylglucosamine, etc. (Nagata et al., 1992). On the other hand, mucosubstances or glycosaminoglycans are composed of mucous and proteins, which mainly contain chondroitin sulfate or heparin, and incorporate the radiosulfate $^{35}SO_4$. Therefore, mucosubstance synthesis can be demonstrated by light and electron microscopy using $^{35}SO_4$ incorporation. We have shown incorporation of radiosulfide into Golgi apparatus and mucigen granules of colonic goblet cells (Nagata et al., 1988a). The half life of ^{35}S is very short, only 87 days, so that experiments should be finished within a few months.

5.1.5. Lipid synthesis

The lipids are esters of high fatty acids and can be classified into simple lipids and compound lipids. The former are composed of glycerol and fatty acids, while the latter are composed of both lipids and other components such as phosphates, glucides or proteins. In order to demonstrate lipid synthesis by light and electron microscopic radioautography, incorporations of either ^{3}H-glycerol or ^{3}H-fatty acids were examined (Nagata et al., 1988b, 1990).

5.2. Small molecular compounds

Small molecular compounds such as precursors of macromolecular compounds (Table 5), hormones and neurotransmitters, vitamins, inorganic compounds, drugs or toxins cannot be demonstrated by wet-mounting radioautography. They are only demonstrable by means of dry-mounting radioautography (Nagata, 1994a).

6. Applications to organ systems

The results obtained from the applications of various precursors or tracers to all the organ systems should be described according to the conventional order of the histology of the organs. The results should be designated as the histochemistry of the organs (Nagata, 1995d).

6.1. The organ of movement

6.1.1. Bones and joints

When 8 groups of salamander larvae at 4, 6, 8 weeks and 12 months after hatching were injected with ^{3}H-thymidine and both the forelimbs and hindlimbs were radioautographed, the aging changes of DNA synthesis demonstrated that the labeling indices of chondrocytes in digital bones showed peaks at 4 weeks then decreased from 6 weeks reaching 0 at 8 months (Kobayashi et al., 1995). We also studied the DNA, RNA and protein synthesis of normal and rheumatoid synovial membranes which were obtained surgically from rheumatoid patients and radioautographed by labeling in vitro with ^{3}H-

Table 5. Quantitative evaluation of soluble ^{3}H-labeled nucleic acid precursors in subcellular compartments demonstrated by dry-mounting radioautography.

PRECURSORS	CELL ORGANELLE	WET-MOUNTING RAG	DRY-MOUNTING RAG	SOLUBLE COMPOUNDS
^{3}H-thymidine				
	Karyoplasma	+++	++	+
	Nucleolus	+	-	+
	Mitochondria	+	+	+
	Endoplasmic reticulum	+	-	+
	Ribosomes	+	-	+
	Golgi complex	+	-	+
	Cytoplasmic matrix	+	-	+
^{3}H-uridine				
	Karyoplasm	++	+	+
	Nucleolus	+++	++	+
	Mitochondria	+	+	+
	Endoplasmic reticulum	++	+	+
	Ribosomes	++	+	+
	Golgi complex	+	-	+
	Cytoplasmic matrix	+	-	+

thymidine, -uridine and -leucine and found no significant difference between the normal and rheumatoid tissues (Kobayashi and Nagata, 1994).

6.1.2. Skeletal muscles

The DNA synthesis of mouse intercostal muscles from prenatal day 13 through postnatal 24 months was studied by ^{3}H-thymidine radioautography, revealing chronological changes of labeling indices reaching a peak at embryo day 13 and decreasing gradually to 0% at 3 months after birth (Hayashi and Nagata, 1993). When rat muscles were injured and labeled with ^{3}H-thymidine, satellite cells were labeled showing that the regenerating muscle fibers originated from satellite cells (Sakai et al., 1977). In the muscles of dystrophy chickens, ^{3}H-thymidine was also incorporated into the satellite cells demonstrating the regeneration by these cells (Oguchi and Nagata, 1981). As for the incorporation of ^{3}H-taurine, however, no difference was found between normal and dystrophy mice by chemical fixation and wet-mounting radioautography (Terauchi et al., 1988). When ^{3}H-taurine was administered to normal or dystrophy mice (518 kBq/g body weight) and their skeletal muscles were observed by freeze-substituted or freeze-dried specimens followed by dry-mounting radioautography, silver grains appeared on sarcoplasmic reticulum, myofilaments, mitochondria and sarcoplasmic membranes (Terauchi and Nagata, 1993). More silver grains were observed in normal mice than dystrophy mice. Only a few silver grains were observed in the specimens which were fixed with conventional glutaraldehyde and osmium tetroxide fixation followed by wet-mounting radioautography. From the results, it is concluded that ^{3}H-taurine is diffusible and is associated with skeletal muscle cells. Taurine is an amino acid which regulates intracellular calcium transport and excitability of cell membrane.

6.2. The circulatory organs

Among the cardiovascular organs, the spleen, some blood cells and blood vessels were studied in our laboratory.

6.2.1. The artery

The localization of calcium antagonists, ^{3}H-benidipine hydrochloride and ^{3}H-nitrendipine, as antihypertensive drugs, was studied in the arteries of spontaneously hypertensive rats by conventional wet-mounting radioautography and cryo-fixed dry-mounting radioautography. The results showed that the silver grains by both drugs mainly localized over the plasma membranes and the cytoplasm of the smooth muscle cells in the tunica media of the mesenteric arteries, suggesting the pharmacological active sites of these drugs (Suzuki et al., 1994).

6.2.2. The blood cells

DNA synthesis of myeloma cells obtained from a human myeoloma patient (Fujii et al., 1980) and DNA, RNA and mucosubstance synthesis of mastocytoma and mast cells from rats (Murata et al., 1977, 1978) were studied by ^{3}H-thymidine, ^{3}H-uridine and $^{35}SO_4$ radioautography, demonstrating incorporation changes of those abnormal cells from normal cells.

Concerning the drug localization in the blood cells, Tranilast distribution was studied. Tranilast is a synthetic anti-allergic agent, synthesized by Kissei Pharmaceutical Co. in Japan. Its chemical structure is N-(3, 4-dimethoxycinnamoyl) anthranilic acid, which was labeled with ^{3}H by NEN, Boston, MA, USA (specific activity 16.0 GBq/mM). When mast cells were collected from Wistar rat peritoneal fluid and labeled in vitro for 60 minutes in PBS containing ^{3}H-tranilast (3.7 MBq/ml) and fixed and radioautographed by wet-mounting, light

and electron microscopic radioautograms showed accumulation of silver grains over mast cell granules, suggesting the inhibition of degranulation of mast cells for anti-allergic reaction (Nagata et al., 1986; Nishigaki et al., 1987).

6.2.3. The spleen

The spleen cells from various stages of aging ddY mice were examined by light and electron microscopic ^{3}H-thymidine radioautography combined with the acid phosphatase activity. The aging changes of DNA synthesis (Olea and Nagata, 1992a) as well as RNA synthesis (Olea and Nagata, 1992b) of the spleen cells were demonstrated.

6.3. The digestive organs

Many papers have been published from our laboratory dealing with the macromolecular synthesis of respective digestive organs from the oral cavity to the gastrointestinal tract and digestive glands (Nagata, 1995a). The results should be described in the order of systematic anatomy and special histology.

6.3.1. The oral cavity

Light and electron microscopic radioautographic studies with ^{3}H-thymidine were carried out on DNA synthesis of mucosal epithelium of the tongue and submandibular glands of aging mice from fetal day 19 to postnatal 2 years. The results showed that the labeling indices of respective cell types in the submandibular glands increased from fetal to postnatal day 1 and then steadily decreased to 2 years. Among respective cell types, the intercalated duct cells were the most frequently labeled and persisted for a longer period. The results suggested that intercalated duct cells are involved with the proliferation of other cell types (Chen et al., 1995).

6.3.2. The esophagus

The DNA synthesis of the esophagus of aging mice labeled with ^{3}H-thymidine were studied by light and electron microscopy (Duan et al., 1992, 1993). The labeled cells were mainly found in the basal layer of the esophageal epithelium. By electron microscopy the nuclei and nucleoli of labeled cells were larger than those of unlabeled cells, but contained fewer cell organelles (Duan et al., 1992, 1993). The labeling indices in respective aging groups showed a peak at 1 day after birth and decreased with aging (Duan et al., 1993).

6.3.3. The stomach

The turnover of fundic glandular cells by ^{3}H-thymidine radioautography was extensively investigated by Leblond and co-workers (Leblond, 1981). We studied the secretion process in G-cells by electron microscopic ^{3}H-amino acid radioautography. When rat stomach tissues were labeled with ^{3}H-glutamic acid and ^{3}H-glycine in vitro at varying time intervals, silver grains in the radioautograms appeared first over the Golgi zones, then migrated to secretory granules and were stored in the cytoplasm, suggesting the secretory kinetics (Sato, 1978; Sato et al., 1977). We also studied the mechanism of serum albumin passing through the gastric epithelial cells by electron microscopic radioautography. When rat stomach tissues were labeled with ^{132}I-albumin in vitro at varying time intervals, silver grains in the radioautograms appeared over rough endoplasmic reticulum within 3 min, then moved to the Golgi apparatus in 10 min, and on to secretory granules and into the lumen in 30 min, suggesting the pathway of serum albumin from the blood vessels through the gastric mucous epithelial cells into the gastric lumen (Komiyama et al., 1978).

When incorporation of radiosulfate into sulfated complex carbohydrate in rat stomach was studied by labeling with $^{35}SO_4$ in vivo, silver grains appeared over the glandular cells of the pyloric gland but not those of the fundic gland, demonstrating the mucous synthesis in the former glands (Nagata et al., 1988a,b).

6.3.4. The intestines

^{3}H-thymidine radioautography was carried out in the small and large intestines. The cells labeled with ^{3}H-thymidine were localized in the crypts of both small and large intestines, a region defined as the proliferative zone. In the colon of aging mice from fetal to postnatal 2 years, the labeled cells in the columnar epithelia were frequently found in the perinatal groups from embryo to postnatal day 1 (Fig. 4A). However, the labeling indices became constant from the suckling period until senescence (Morita et al., 1993). The labeling indices of respective cell types in each layer such as columnar epithelial cells, lamina propria, lamina muscularis mucosae, tunica submucosa, inner circular muscle layer, outer longitudinal muscle layer, outer connective tissue and serous membrane of the colon and the cecum were examined and it was found that most labeling indices decreased after birth to 2 months except the epithelial cells, which kept a constant value to senescence (Jin, 1995). Similar results were also obtained from the cecum (Fig. 4B; Jin and Nagata, 1995a,b).

On the other hand, the synthesis of mucosubstances in goblet cells as well as in absorptive epithelial cells was studied using $^{35}SO_4$ in the duodenum, jejunum and colon at varying time intervals (Nagata et al., 1988a). The results showed that silver grains over goblet cells in the lower region of the colonic crypt transferred rapidly from 30 to 180 min, while they transferred slowly in goblet cells in the upper region of the colonic crypt, which lead to the conclusion that the rates of transport and secretion of mucous products of the goblet cells at

these two levels in the crypts were different. We also studied the aging changes of ^{3}H-glucosamine uptake in the mouse ileum, and found that the silver grains in the columnar epithelial cells were mainly localized over brush borders and the Golgi region, whereas in the goblet cells they were over the Golgi region and mucous granules. The number of silver grains increased from 6 months up to 2 years due to aging of animals (Morita, 1993).

6.3.5. The liver

Light and electron microscopic radioautography of prenatal and postnatal normal ddY mice at various ages labeled with ^{3}H-thymidine revealed that many silver grains were localized over the nuclei of various cell types constituting the liver, i.e., hepatocytes (Fig. 5A), sinusoidal endothelial cells (Fig. 5A), Kupffer's cells, Ito's fat-storing cells, bile ductal epithelial cells, fibroblasts and hematopoietic cells (Ma, 1988; Ma and Nagata, 1988). In hematopoietic cells, silver grains were observed over the nuclei of erythroblasts, myeloblasts, lymphoblasts and megakaryocytes. However, most hematopoietic cells disappeared on postnatal day 14. At fetal day 19, the liver tissues consisted chiefly of hepatocytes and hematopoietic cells and no lobular orientation was observed. At postnatal day 1 and 3, lobular formation started. The hepatic lobules were formed at day 9 after birth. During the perinatal period, almost all cell types were labeled with ^{3}H-thymidine. The percentage of labeled hepatocytes (labeling index) was highest at fetal day 19, and rapidly decreased after birth to day 3. From day 9 to 14, the labeling index gradually decreased, reaching its lowest point at 24 months. When the labeling indices of hepatocytes in 3 hepatic acinar zones were analyzed, the indices decreased in intermediate zone and peripheral zone on days 3 and 9 after birth, whereas they increased in central zone on day 9, and then completely disappeared from day 14 to 24 months. When the size and number of cell organelles in both labeled and unlabeled hepatocytes on EMRAG were estimated quantitatively by image analysis with an image analyzer, Digigramer G/A (Mutoh Kogyo Co. Ltd., Tokyo, Japan), the area of the cytoplasm, nucleus, endoplasmic reticulum, mitochondria as well as the number of mitochondria in the unlabeled hepatocytes were more than the labeled cells (Ma and Nagata, 1990a). These data demonstrated that the cell organelles of hepatocytes which synthesized DNA were not well developed when compared to those not synthesizing DNA during postnatal development. In some unlabeled hepatocytes, several silver grains were occasionally observed localizing over mitochondria and peroxisomes, as was formerly reported (Nagata et al.,

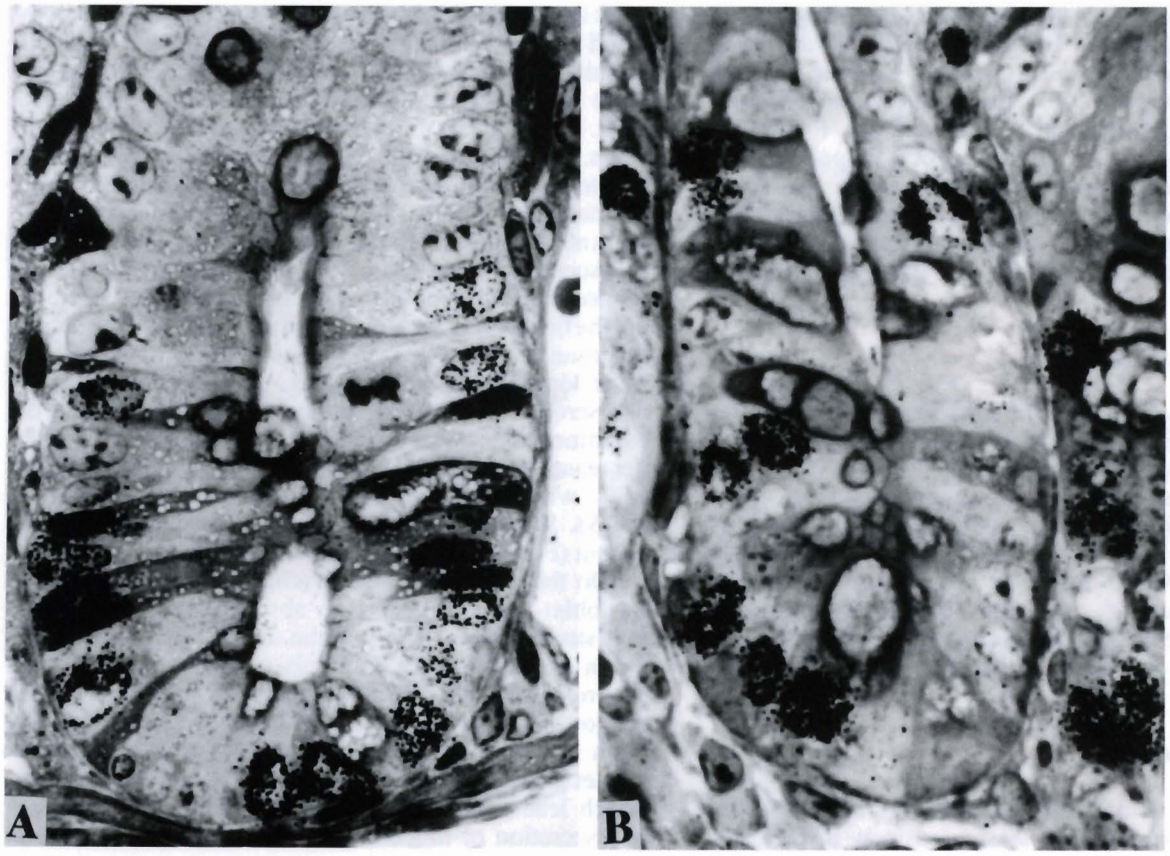

Fig. 4. Light microscopic radioautograms (LMRAG) of the large intestines of mice at various ages injected with ^{3}H-thymidine, demonstrating DNA synthesis. **A.** The proximal colon of an adult mouse at 1 month after birth. Several columnar epithelial cells and vacuolated cells are labeled but not the goblet cells. x1,000. **B.** The cecum of a young mouse at 2 weeks after birth. Silver grains are localized over the nuclei of columnar epithelial cells of the lower half of the crypts. x 1,000

1967b, 1982). The labeling indices of other cell types such as sinusoidal endothelial cells also showed a decrease from the perinatal period to 24 months.

When mice were injected with ^{3}H-uridine, light and electron microscopic radioautograms showed that silver grains were localized over the nucleoli, nuclear chromatin (both euchromatin and heterochromatin), mitochondria and the rough-surfaced endoplasmic reticulum of hepatocytes (Fig. 5B) as well as other types of cells such as sinusoidal endothelial cells, Kupffer's cells, Ito's fat-storing cells, ductal epithelial cells, fibroblasts and hematopoietic cells in the livers at various ages (Ma and Nagata, 1990b). By quantitative analysis, the total number of silver grains in the nucleus, nucleolus and cytoplasm of each hepatocyte increased gradually from fetal day 19, reached the maximum at 14 days of postnatal age, then decreased to 24 months. The number of silver grains in the nucleolus, when classified into two compartments, (grains over granular components and those over fibrillar components), both increased paralelly after birth, reaching their maxima on day 14, then decreased to 24 months with aging. However, when the ratios (%) of silver grains over euchromatin, heterochromatin of the nuclei and granular and fibrillar components of the nucleoli were calculated, the ratios remained constant at each aging point.

When ^{3}H-leucine was injected into mice at various ages silver grains in RAG were observed over all cell types of the liver, i.e. hepatocytes, sinusoidal endothelial cells, ductal epithelial cells, Kupffer's cells, Ito's fat storing cells, fibroblasts and hematopoietic cells (Ma and Nagata, 1991). In hepatocytes, the number of silver grains in cytoplasm and karyoplasm increased from perinatal animals to postnatal 1-month-old animals and decreased with aging to 24 months. The number of silver grains observed over respective cell organelles varied with aging, reaching their maximum at 1 month (Ma et al., 1992).

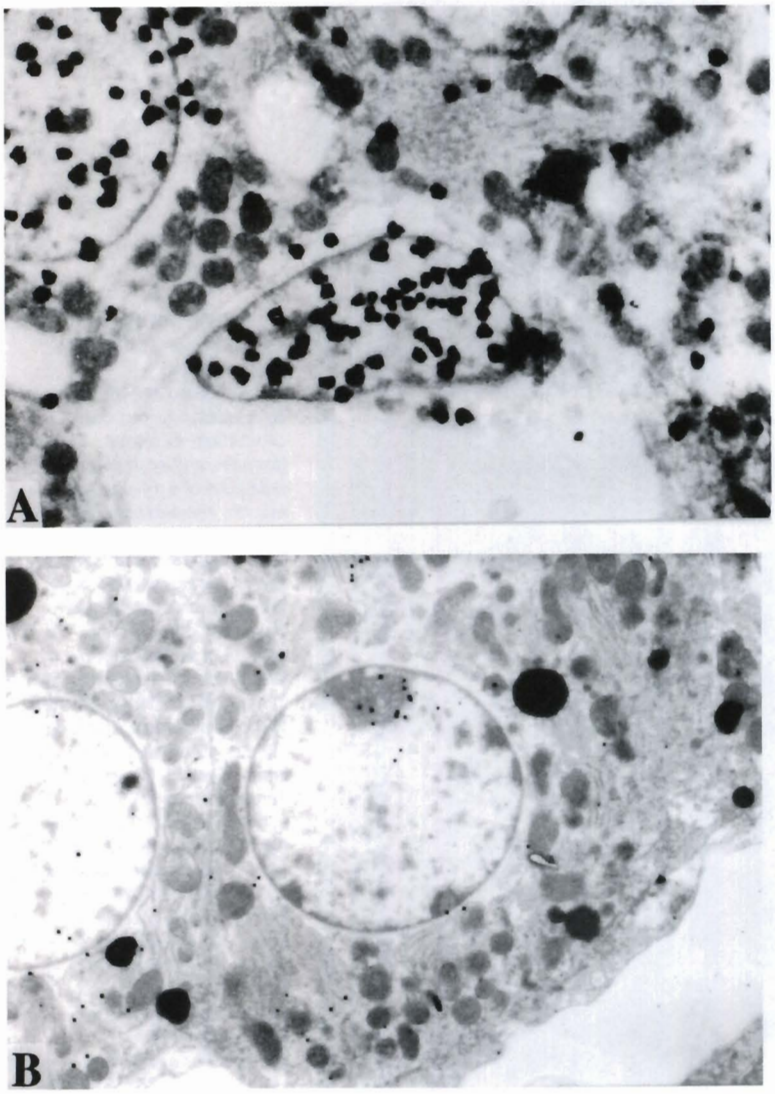

Fig. 5. Electron microscopic radioautograms (EMRAG) of the livers of young mice showing macromolecular synthesis. **A.** The liver of a 14-day-old mouse injected with ^{3}H-thymidine, demonstrating DNA synthesis. Many silver grains are localized over the nucleus of a labeled sinusoidal endothelial cell at the center of the picture and a labeled hepatocyte at upper left corner. x 8,000. **B.** A hepatocyte of a 9-day-old mouse labeled with ^{3}H-uridine, demonstrating RNA synthesis. Many silver grains are mainly localized over the nucleolus and a few over the chromatin and the cytoplasm. x 4,000

Concerning the glucide synthesis, we studied ^{3}H-glucose incorporation into glycogen in the liver, in conjunction with soluble compounds (Nagata and Murata, 1977). Soluble ^{3}H-glucose, which was demonstrated by cryo-fixation and dry-mounting radioautography, was diffusely localized over the nucleus, cell organelles and cytoplasmic ground substance of hepatocyte. By conventional chemical fixation and wet-mounting radioautography, silver grains were localized only over glycogen granules, endoplasmic reticulum and Golgi apparatus.

We also observed lipid synthesis in the liver using ^{3}H-glycerol in conjuntion with soluble compounds (Nagata and Murata, 1977). When adult mice were injected with ^{3}H-glycerol and the livers were cryo-fixed at -196 °C, freeze-substituted embedded in epoxy resin, dry-sectioned, and prepared for dry-mounting radioautography, many silver grains appeared diffusely over the nuclei and cytoplasm. However, when the same liver tissues were fixed chemically in buffered glutaraldehyde

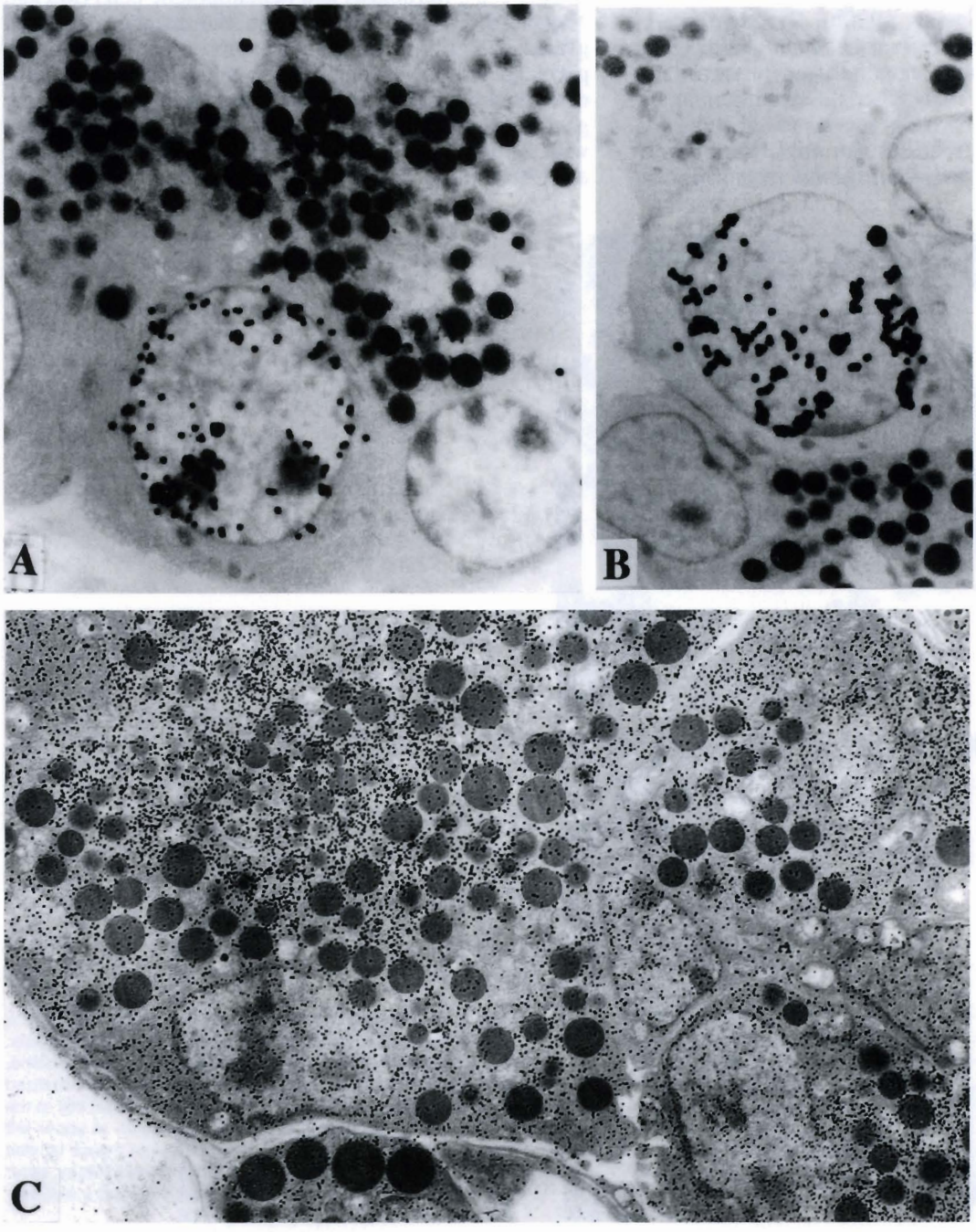

Fig. 6. EMRAG of the pancreases of young mice demonstrating macromolecular synthesis. **A.** A labeled acinar cell containing secretory granules and endoplasmic reticulum of a 14-day-old mouse, injected with ^{3}H-thymidine demonstrating DNA synthesis. Many silver grains are observable over the nucleus at the center. The other cells are not labeled. x 10,000. **B.** A labeled centro-acinar cell of the exocrine terminal portion of the pancreas of a 14-day-old mouse at the center, injected with ^{3}H-thymidine demonstrating DNA synthesis. x 10,000. **C.** The pancreatic acinar cells of a 14-day-old mouse, injected with ^{3}H-glucosamine demonstrating glucide synthesis. Many silver grains are observed over the nuclei, nucleoli, endoplasmic reticulum, Golgi apparatuses, secretory granules and cytoplasmic matrix. x 8,000

and osmium tetroxide and radioautographed by conventional wet-mounting procedures, very few silver grains were observed except over the endoplasmic reticulum and lipid droplets, which demonstrated macromolecular lipid synthesis.

As for the drug distribution in the liver, intracellular localizations of a few drugs were investigated. Tranilast is a synthetic anti-allergic agent and its chemical structure is N-(3, 4-dimethoxycinnamoyl) anthranilic acid. When the livers of Wistar rats administered orally with ^{3}H-tranilast were observed by light microscopic RAG, many silver grains were seen over the hepatocyte nuclei and cytoplasm. The grain counts reached maximum at 3 hours after administration, which suggested metabolic process of Tranilast from uptake to excretion in the liver (Momose et al., 1989). Intracellular localization of a peroxisome proliferator, 14 °C-labeled bezafibrate was also demonstrated in cultured rat hepatocytes by light and electron microscopic radioautography (Momose and Nagata, 1993; Momose et al., 1995). About 90% of all the silver grains were localized over the cytoplasm. On electron microscopic radioautograms of whole-mount cultured cells, silver grains were localized on cytoplasmic matrix, especially over the endoplasmic reticulum. The results showed that the receptor of peroxisome proliferator should be associated with the endoplasmic reticulum (Momose et al., 1995).

6.3.6. The pancreas

Light end electron microscopic radioautograms of the pancreas revealed that the nuclei of pancreatic acinar cells (Fig. 6A), centro-acinar cells (Fig. 6B), ductal epithelial cells, and endocrine cells were labeled with ^{3}H-thymidine. The labeling indices of these cells peaked on day 1 after birth and decreased gradually to 24 months (Nagata et al., 1984). Light and electron microscopic radioautograms of mouse pancreas, injected with ^{3}H-uridine, demonstrated incorporation of ^{3}H-uridine into exocrine and endocrine cells (Nagata and Usuda, 1986). The silver grains were found more in pancreatic acinar cells than in ductal or centro-acinar cells. Among the acinar cells, the number of silver grains increased after birth to day 14, then decreased with aging. Quantification of silver grains in the nucleoli, chromatin, and cell body was carried out by X-ray microanalysis, which verified the results obtained by visual grain counting (Nagata, 1991, 1993a; Nagata and Usuda, 1986).

Incorporation of ^{3}H-leucine into endoplasmic reticulum, Golgi apparatus and to the secretory granules of pancreatic acinar cells was first demonstrated by Jamieson and Palade (1967). We have studied ^{3}H-glycine incorporation into these cell organelles of mouse pancreatic acinar cells in conjunction with soluble compounds (Nagata and Murata, 1977). The quantitative aspects of protein synthesis using ^{3}H-leucine in regard to aging have also been clarified, showing an increase of silver grain numbers after birth, reaching a peak from 2 weeks to 2 months and a decrease to 2 years (Nagata, 1993b; Nagata and Usuda, 1993).

As for glucides synthesis, we studied incorporation of ^{3}H-glucosamine into the glycoproteins of the pancreas of aging mouse at various ages by light and electron microscopic radioautography (Nagata et al., 1992). When perinatal baby mice received ^{3}H-glucosamine injections and the pancreatic tissues were radioautographed, silver grains were observed over exocrine and endocrine pancreatic cells. However, these silver grains were few in number. When juvenile mice at the age of 14 days after birth were examined, many silver grains appeared over the exocrine pancreatic acinar cells (Fig. 7C), with fewer silver grains observed over endocrine pancreatic cells and ductal epithelial cells. The grains in

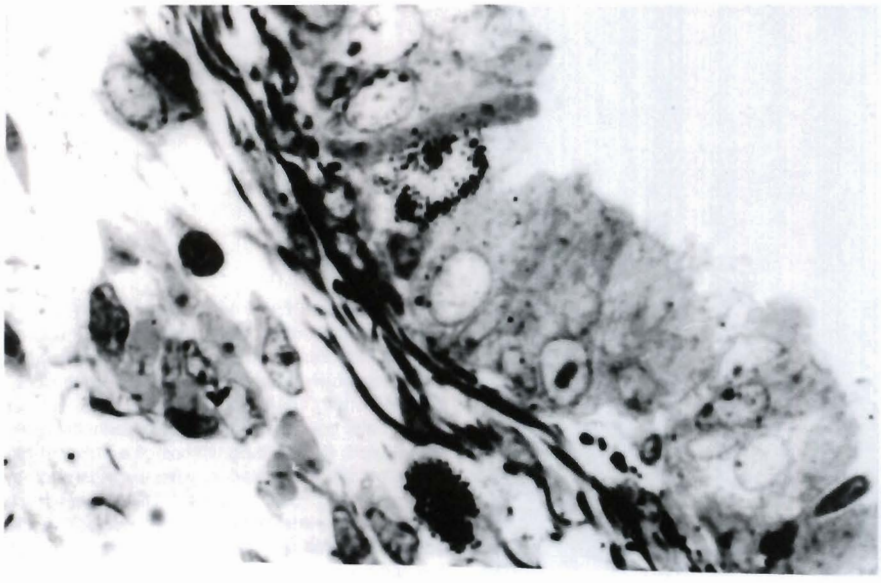

Fig. 7. LMRAG of the trachea of a young mouse at 1 week after birth, labeled with ^{3}H-thymidine in vitro, demonstrating DNA synthesis. Silver grains are localized over the nuclei of ciliated epithelial cells and fibroblasts in the propria mucosa. x 1,000

the exocrine pancreatic acinar cells were localized over the nucleus, endoplasmic reticulum, Golgi apparatus and secretory granules, demonstrating glycoprotein synthesis. Adult mice at 1 or 6 months of age and senile mice at 12 or 24 months showed very few silver grains on radioautograms. Thus, glucide synthesis in the pancreas of mice revealed quantitative changes, i. e., an increase and a decrease of ^{3}H-glucosamine incorporation with aging.

When litters of ddY mice at fetal day 19, postnatal days 1, 3, 7, 14, and postnatal months 1, 2, 6 up to 12 months, were injected with ^{3}H-glycerol and the pancreases were prepared for light and electron microscopic radioautography, silver grains were observed in both exocrine and endocrine cells of respective ages (Nagata et al., 1988a,b, 1990). In perinatal animals from fetal day 19 to postnatal days 1, 3, and 7, cell organelles were not well developed in exocrine and endocrine cells and the number of silver grains was very low. In 14 day old juvenile animals, cell organelles such as endoplasmic reticulum, Golgi apparatus, mito-chondria and secretory granules were well developed and many silver grains were observed over these organelles and nuclei in both exocrine and endocrine cells. The number of silver grains was higher in exocrine than in endocrine cells. In adult animals of 1, 2, and 6 months, the number of silver grains remained constant. In 12-month-old senescent animals, silver grains were fewer than in younger animals. The number of silver grains expressed the degree of lipid synthesis, which increased from the perinatal to the adult period and decreased to senescence.

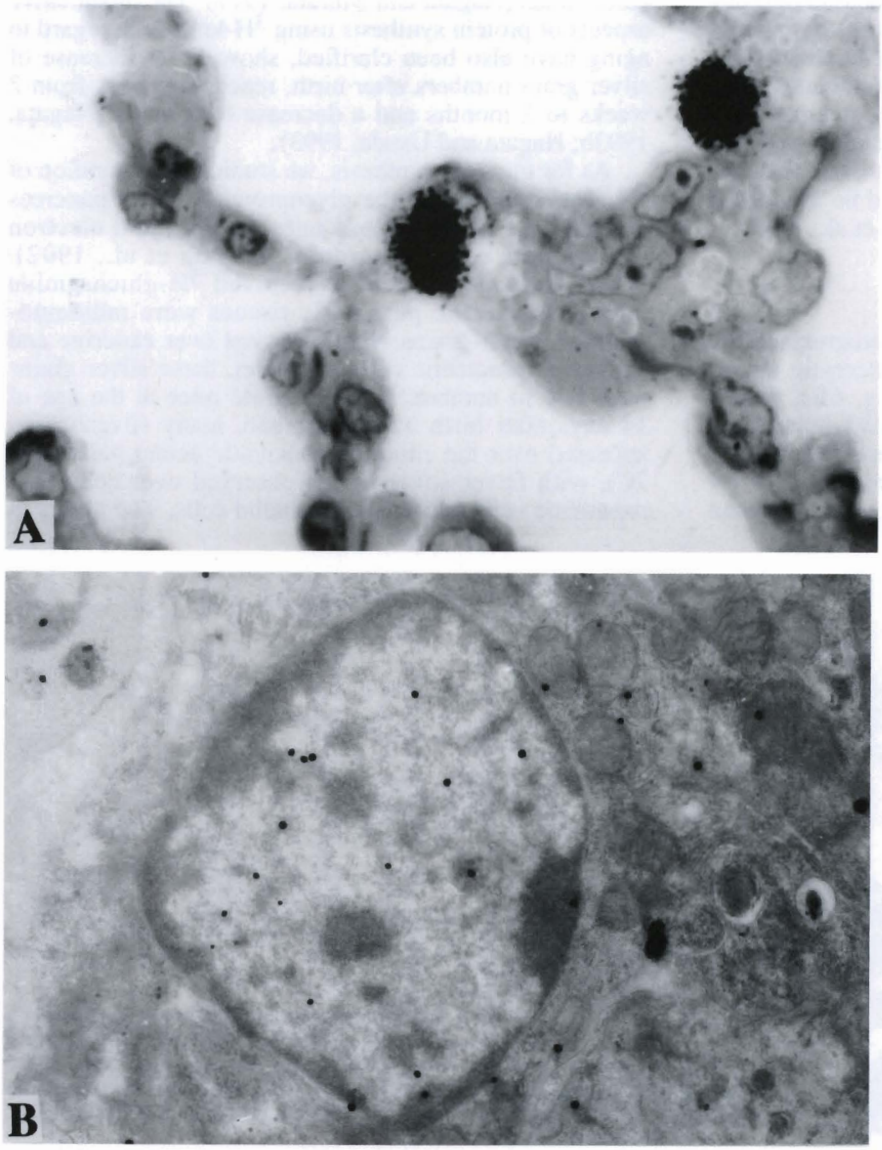

Fig. 8. LM- and EM-RAG of the lungs of young mice demonstrating macromolecular synthesis. **A.** The lung tissue of a mouse at 2 weeks after birth, incubated in vitro with 3H-thymidine, demonstrating DNA synthesis. x 1,100. Two of the alveolar cells, which are type 1 epithelial cells, are labeled. **B.** The lung tissues of a 1-month-old adult mouse, incubated in vitro with ^{3}H-uridine, demonstrating RNA synthesis. Silver grains are observed over the chromatin and nucleoli in the nucleus as well as over the mitochondria in the cell body. x 10,000

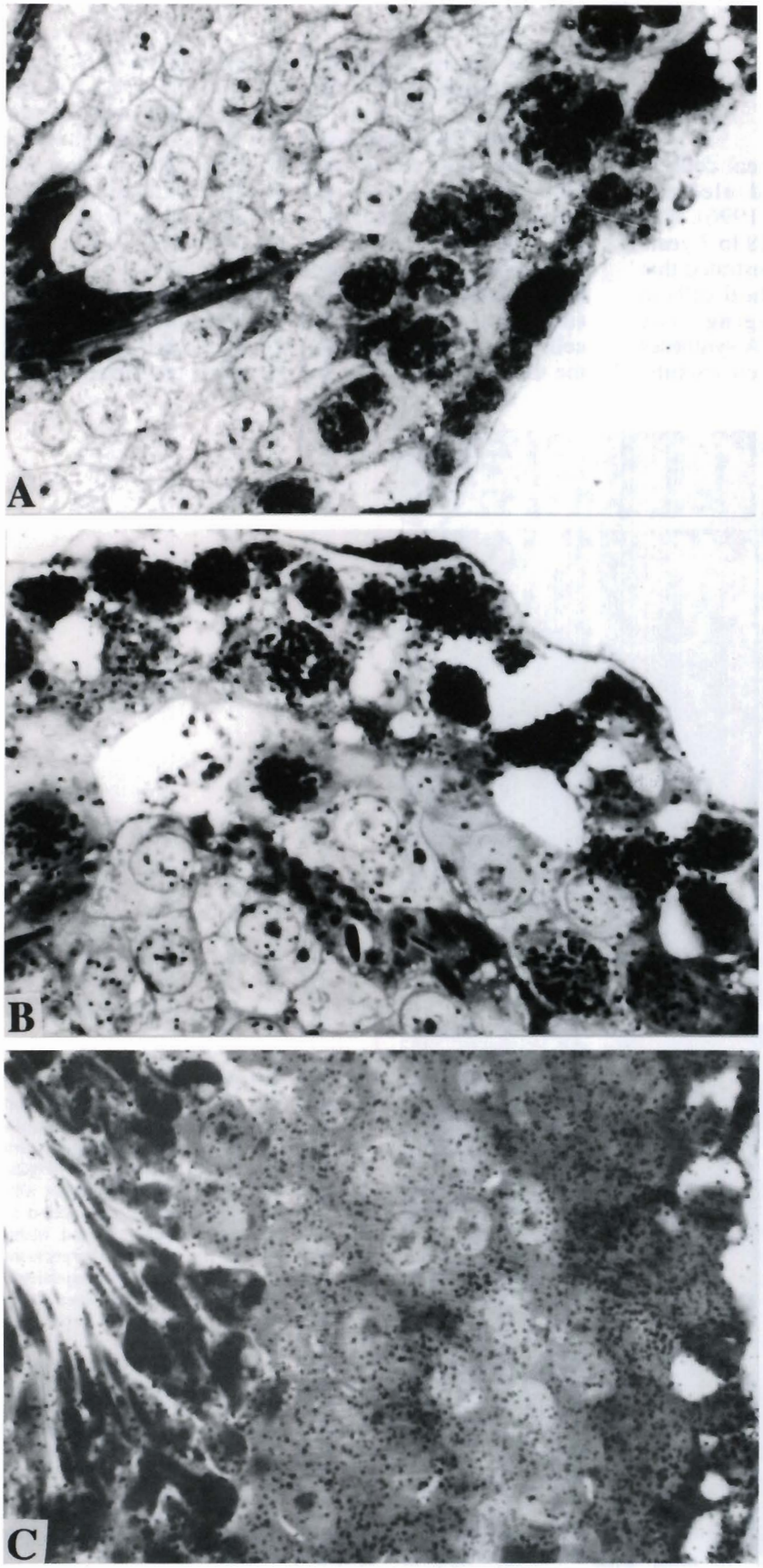

Fig. 9. LMRAG of the testis of aging male mice demonstrating macromolecular synthesis. **A.** A cross section of a seminiferous tubule of the testis of an old male mouse at 1 year after birth, injected with ^{3}H-thymidine, demonstrating DNA synthesis. x 1,100. Many nuclei of the spermatogonium (left) are labeled. x 1,000. **B.** The testis of an old male mouse at 2 year after birth, injected with ^{3}H-uridine, demonstrating RNA synthesis. x 1,100. Many silver grains can be seen over all the nuclei and cell bodies of the spermatogonium (upper half of the picture) as well as the spermatocytes (lower half) are labeled. x 1,000. **C.** The testis of an old male mouse at 1 year after birth, injected with ^{3}H-leucine, demonstrating protein synthesis. x 1,100. Many silver grains are observed over all the nuclei and cell bodies of all the cells, including the spermatogonia (left) and the spermatocytes (right side) in the seminiferous tubule. x 1,000

6.4. The respiratory organs

6.4.1. The trachea

The changes of DNA synthesis of tracheal cells in aging mice were studied by light and electron microscopic radioautography (Sun et al., 1996). The tracheae of 8 groups of mice from fetal day 18 to 2 years after birth were examined. The results demonstrated that the DNA syntheses and morphology of tracheal cells in the mouse tracheae changed due to aging. The radioautograms (Fig. 7) revealed that the DNA syntheses of the nonciliated and basal cells reached their maxima on fetal day 18, then fell from postnatal day 3. Activity of DNA synthesis of ciliated cell was observed but was very low in the fetal stage. Ciliated cell cannot synthesize DNA and proliferate in the postnatal stage. They are supposed to be derived from the division and transformation of basal cell. On the other hand, the DNA synthesis of chondrocytes was highest on embryonic day 18, and rapidly declined on postnatal day 3. The chondrocytes lost the ability to synthesize DNA at 2 months after birth. The DNA syntheses of other cells (including fibroblasts, smooth muscle and glandular cells) were highest on fetal day 18 and fell markedly on the third day after birth and decreased progressively due

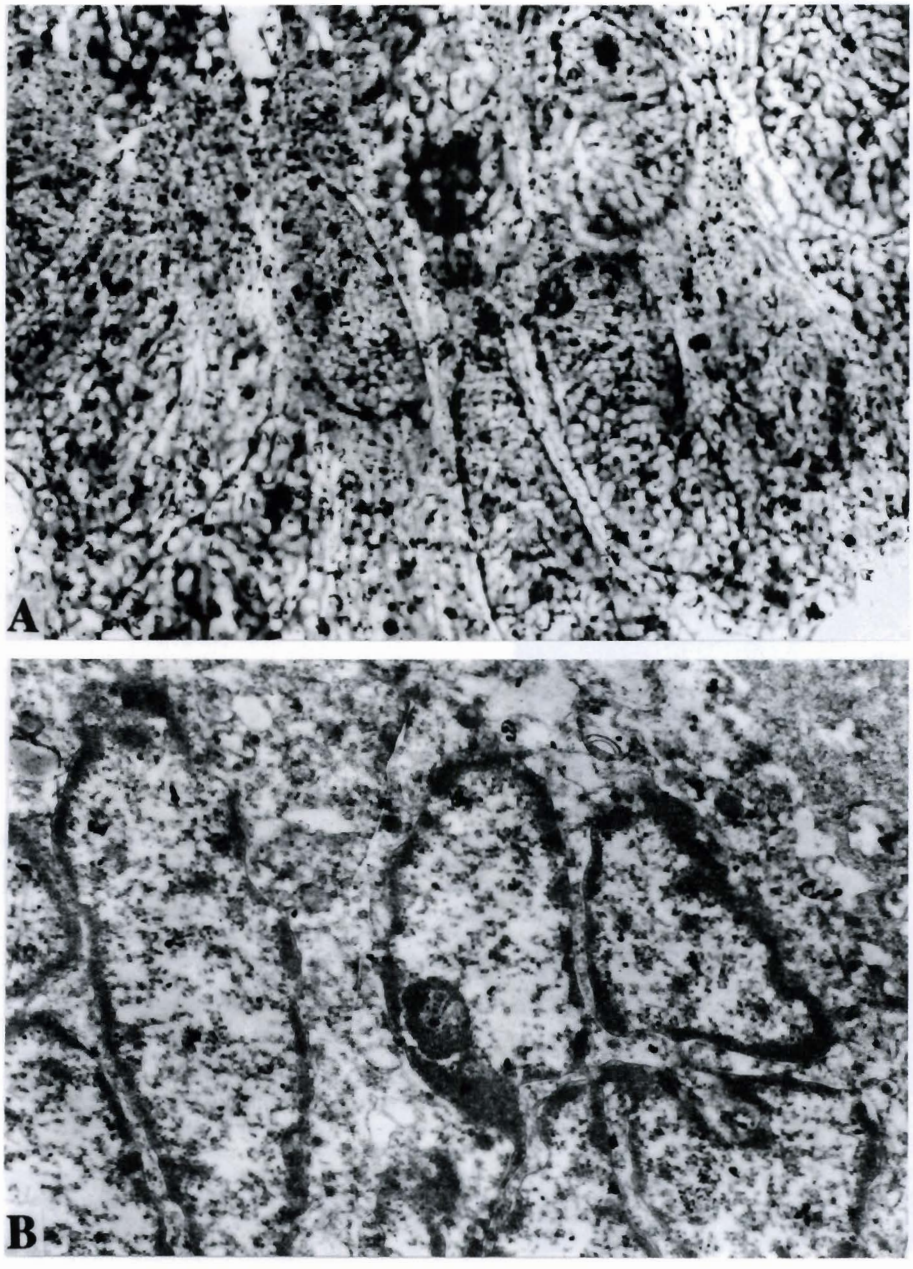

Fig. 10. EMRAG of thyroid cancer cells biopsied from a human patient and incubated in vitro with $^{203}HgCl_2$, showing soluble compounds. **A.** Dry-mounting radioautogram of thyroid cancer cells labeled with $^{203}HgCl_2$ in vitro, cryo-fixed in iso-pentane cooled with liquid nitrogen, freeze-dried, embedded in Epon, dry sectioned and dry-mounted. Many silver grains can be seen over the karyoplasm and cytoplasm of all the cells, showing soluble $^{203}HgCl_2$. x 6,000. Note that the silver grains in both Figs. 10A and 10B appear larger than the other EMRAG (Figs. 5-9, 11-12, 14), because the specimens in Figs. 10 were developed in SD-X1 developer while the others in GL-phenidon developer. **B.** Wet-mounting radioautogram of the same cancer cells as in Fig. 10A, but fixed chemically with glutaraldehyde and osmium tetroxide, dehydrated, embedded in Epon, wet-sectioned and wet-mounted. Only a few silver grains are observable in the karyoplasm and cytoplasm. x 6,000.

to aging. The incorporation of $^{35}SO_4$ of the trachea in aging mice was also studied. Many silver grains were observed over the chondrocytes and extracellular matrix of the tracheal cartilage in fetal and postnatal newborn mice. The number of silver grains was the highest at 2 weeks after birth and decreased rapidly after 1 month (Nagata et al., 1980).

6.4.2. The lung

The lung tissues of aging mice were labeled with ^{3}H-thymidine and observed by light and electron microscopic radioautography (Sun et al., 1994, 1995). As a result, respective cell types of the lung, cuboidal epithelial cells (type 1 epithelial cells), interstitial cells and endothelial cells were labeled (Fig. 8A) and their labeling indices were different. The labeling indices of cuboidal epithelial cells (47%), interstitial cells (38%), and endothelial cells (29%) were found to peak on fetal day 18 and postnatal day 1. Then, a second peak appeared on postnatal day 3, after which the index decreased with aging. The aging changes of DNA synthesis in the lungs of salamanders from larvae (2 month after fertilization), juvenile (1 month), adults (10 and 12 months after metamorphosis) to senescence (5 years) were studied by LMRAG (Matsumura et al., 1994). The results showed that the labeling indices in the ciliated cells and mucous cells in the superficial layer of young animals were higher than those of the basal cells and they decreased in adults, demonstrating aging changes in salamanders.

When the lung tissues of mice were labeled with ^{3}H-uridine, RNA synthesis was observed in all cells of the lung at various ages (Sun, 1995). The number of silver grains changed with aging. The grain counts in type 1 epithelial cells increased from the 1st day after birth and reached a peak at 1 week, while the counts in type 2 epithelial cells (Fig. 10B) and interstitial cells increased from embryo day 16 and reached peaks at 1 week after birth. They diminished with the developing of the lung with aging. On the other hand, inhalation experiment of ^{3}H-thymidine by means of a nebulizer into the lungs of 1 week old mice was carried out. After 45 min inhalation, the lung tissues were taken out and processed by either rapid-freezing and freeze-substitution for dry-mounting radioautography or conventional chemical fixation for wet-mounting radioautography. By wet-mounting RAG silver grains were observed in the nuclei of a few alveolar type 2 cells and interstitial cells, demonstrating DNA synthesis. By dry-mounting RAG numerous silver grains were located diffusely over all the epithelial cells and interstitial cells, demonstrating soluble compounds (Duan et al., 1994).

6.5. The urinary organs

6.5.1. The kidney

The DNA synthesis by ^{3}H-thymidine radioautography as well as PCNA/cyclin immunohistochemistry were studied in ddY aging mice from prenatal day 13 to postnatal year 1 (Hanai, 1993; Hanai et al., 1993). The labeling indices by light microscopic radioautography as well as the PCNA/cyclin-positive indices in glomeruli (28 to 32%) and uriniferous tubules (31 to 33%) in the superficial layer were higher than those (10 to 12%) and (8 to 16%) in the deeper layer from the late fetal to the suckling period, then they decreased from weanling to senescence with aging. Electron microscopic radioautography revealed the same results (Hanai and Nagata 1994a,b). The number of silver grains demonstrating the incorporation of ^{3}H-uridine in glomeruli (34.6 per cell) and uriniferous tubules (56.4 per cell) were higher in the superficial layer than those (15.6 and 18.6 per cell) in the deeper layer at embryonic day 15 and decreased gradually with aging (Hanai and Nagata 1994b). The incorporations of ^{3}H-glucosamine in the kidney of aging mice demonstrated by light and electron microscopic RAG revealed that the number of silver grains in both the glomeruli and uriniferous tubules were less in the embryonic stage, but increased postnatally and reached peaks at 1 to 2 weeks then decreased to senescence (Joukura and Nagata, 1995).

6.5.2. The urinary bladder

The urinary bladders of rats were investigated by light microscopic radioautography after oral administration of ^{3}H-tranilast, an anti-allergic agent. It was found that this agent specifically localized over the transitional epithelial cells and endothelial cells of the veins in the mucosa for a long time, which suggested the relationship between the histopathology of the cystitis observed after the administration of the drug in human patients (Nishigaki et al., 1990).

6.6. The genital organs

6.6.1. The male genital organs

Macromolecular synthesis in aging mouse testis by light and electron microscopic radioautography revealed incorporations of ^{3}H-thymidine, ^{3}H-uridine and ^{3}H-leucine into various cells of the seminiferous tubules (Gao, 1993; Gao at al., 1994). At embryonic and neonatal stages, myoid cells and Sertoli's cells labeled with ^{3}H-thymidine were frequently observed, whereas from young adulthood to senescence the labeling indices of both cells decreased. However, DNA synthesis of gonocytes started 4 days after birth, and the labeling index of spermatogonia first peaked at 3 weeks and stayed constant until senescence (Fig. 9A). The DNA synthesis in Leydig cells, on the contrary, increased throughout adult stages and did not decrease until senescence (Gao et al., 1995a,b). On the other hand, the RNA synthesis (Fig. 9B) and protein synthesis (Fig. 9C) of various cells in the seminiferous tubules were weak at the embryonic and neonatal stages. The grain counts

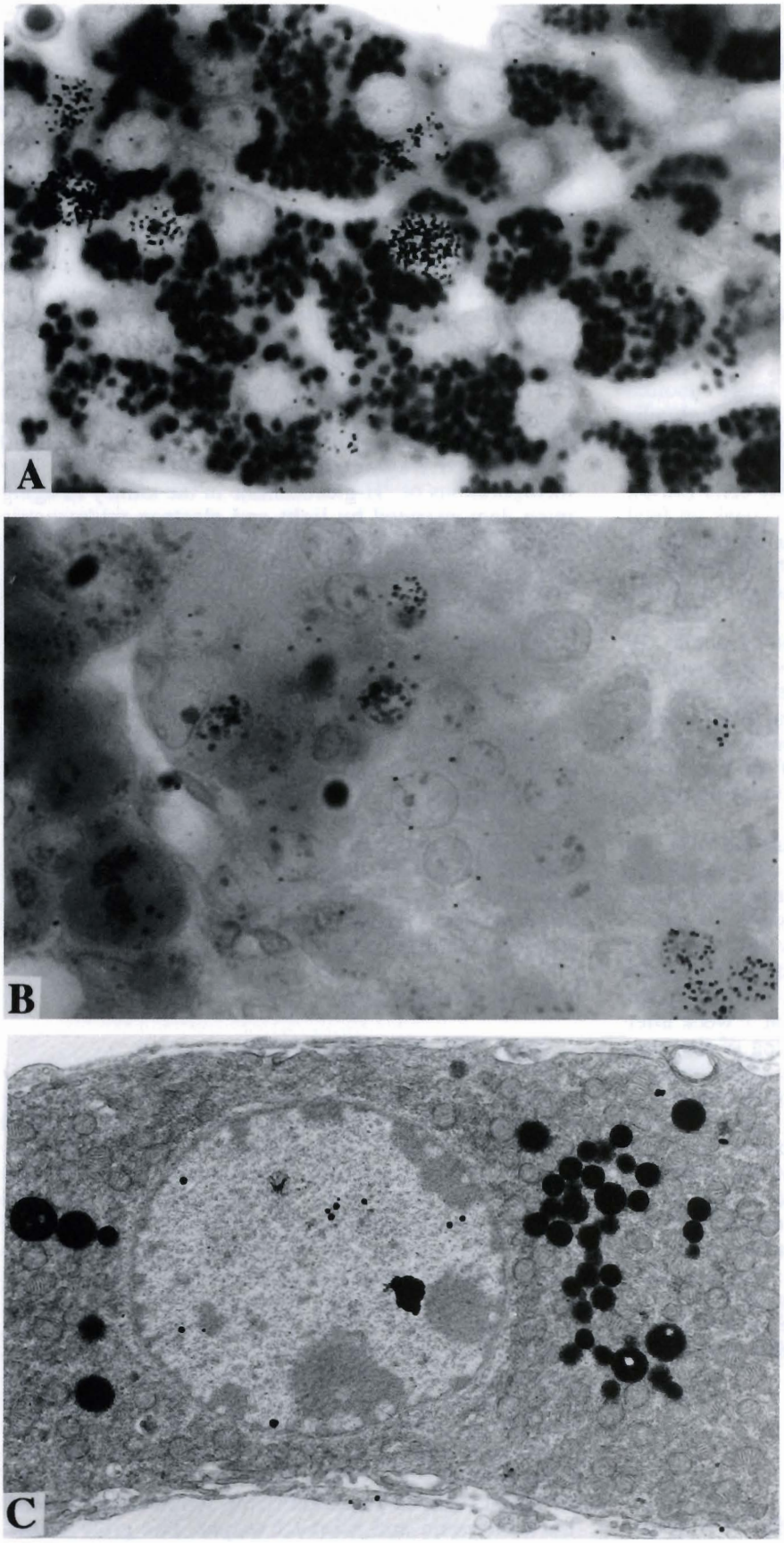

Fig. 11. LM- and EM-RAG of the adrenals of perinatal mice injected with ^{3}H-thymidine, demonstrating DNA synthesis. **A.** LMRAG of the adrenal cortex of a fetal day 19 embryo. Many silver grains are localized over several nuclei of the cortical cells in the zona fasciculata. x 800. **B.** LMRAG of the adrenal cortex and medulla of a fetal day 19 embryo. Both the zona reticularis (left) and the medulla can be seen in the picture. Many silver grains are localized over several nuclei of the medullary cells. x 800. **C.** EMRAG of a young mouse at postnatal day 14. Several silver grains can be seen over the nucleus of a cell in the zona fasciculata. x 6,000

with ^{3}H-uridine and ^{3}H-leucine increased at adult stages and maintained high levels until senescence (Gao, 1993).

6.6.2. The female genital organs

6.6.2.1. The ovary. The mucosubstance synthesis with radiosulfate, $^{35}SO_4$, was studied in the ovaries of mice during the estrus cycle. Four groups of female ddY, aged 8-10 weeks, were divided into 4 groups, diestrus, proestrus, estrus and metestrus, according to the vaginal smears. The ovaries were taken out, labeled with $^{35}SO_4$ in vitro and radioautographed. In all the animals, silver grains were localized over the granulosa and theca cells. Almost all compartments of the ovary were labeled. The grain counts per cell changed according to cell cycle. From the results, it was concluded that all the cells of the ovary incorporated mucosubstances throughout the estrus cycle (Li et al., 1992).

6.6.2.2. The uterus. The DNA and RNA syntheses in the developing virgin mouse ovary and oviduct were studied by ^{3}H-thymidine and ^{3}H-uridine radioautography. Both DNA and RNA incorporations were active in all surface epithelial, stromal and follicular cells of the

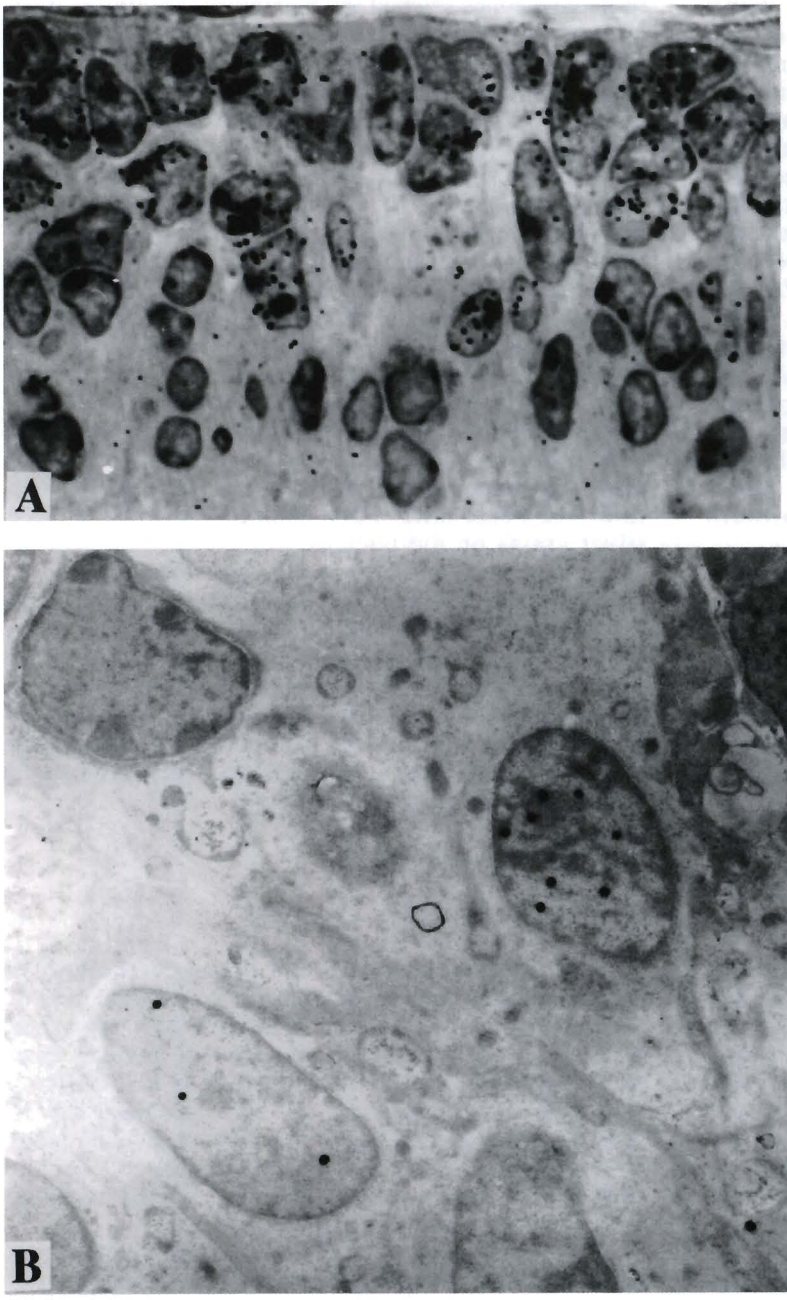

Fig. 12. LM- and EM-RAG of the cerebella of newborn mice injected with ^{3}H-thymidine, demonstrating DNA synthesis. **A.** LMRAG of the cerebellum of a mouse at 3 days after birth, showing external granular layer. Many labeled neuroblasts are observable in the outermost 4-5 rows demonstrating DNA synthesis, while the nuclei in the innermost 1-3 rows are not labeled. x 1,800. **B.** EMRAG of the cerebellum of a mouse at 8 days after birth, showing DNA synthesis in the neuroblasts in the external granular layer. Two of the nuclei are labeled with several silver grains. x 10,000

ovary between postnatal days 1 to 7 and decreased from day 14 on. However, DNA synthesis of the uterus was active at days 1 and 3 and decreased from day 7, while RNA synthesis of the uterus increased from day 1 to 14 and decreased from day 30 to 60 (Li, 1994; Li and Nagata, 1995).

On the contrary, in order to detect the changes of DNA, RNA and protein synthesis in the mouse endometrium during activation of implantation, ovulations of female BALB/C strain mice were controlled by pregnant mare serum gonadotropin and human chorionic gonadotropin. Then, pregnant female mice were ovariectomized on the 4th day of pregnancy. The delay implantation state was maintained for 48 hrs and after 0 to 18 hrs of estrogen supply, ^{3}H-thymidine, ^{3}H-uridine and ^{3}H-leucine were injected respectively. Three regions of the endometrium, i. e. the interinplantation site, the antimesometrial and mesometrial sides of the implantation site, were processed for light and electron microscopic radioautography. The cells labeled with ^{3}H-thymidine increased after nidatory estradiol effects in the stromal cells around the blastocyst, but not in the epithelial cells (Yamada and Nagata, 1992a). The cells labeled with ^{3}H-uridine (Yamada and Nagata, 1992b) and ^{3}H-leucine (Yamada, 1993) increased, reaching a peak at 6 hrs after estrogen induction in both the stromal and epithelial cells on the antimesometrial side. The results suggested that the presence of the blastocyst in the uterine lumen induced selective changes in the behavior of endometrial cells after nidatory estradiol effect showing the changes of DNA, RNA and protein synthesis.

On the other hand, collagen synthesis in the mouse decidual cells was studied by light and electron microscopic radioautography using ^{3}H-proline. Silver grains were localized over the endoplasmic reticulum and Golgi apparatus of fibroblasts and accumulated over collagen fibrils in the extracellular matrix. The results suggested that the decidual cells produced collagen in the matrix (Oliveira et al., 1991, 1995).

6.7. The endocrine organs

6.7.1. The thyroid

Normal human thyroid tissues and thyroid cancer tissues obtained from struma patient by surgery were labeled in vitro with $^{203}HgCl_2$ and processed through both conventional chemically-fixed wet-mounting radioautography and freeze-dried dry-mounting radioautography. The results revealed that numerous silver grains showing soluble component of mercury were found diffusely in thyroid cancer cells (Fig. 10A) but less silver grains showing insoluble component (Fig. 10B) were observed in cancer and normal thyroid cells (Nagata et al., 1977c). The results supported the concentration of hot mercury in the thyroid cancer cells in the struma patients.

6.7.2. The adrenal gland

Incorporation of ^{3}H-thymidine was observed in aging mouse adrenal gland from embryo to postnatal newborn, young, and 2-year-old adult senescent by light and electron microscopic radioautography (Ito, 1995; Ito and Nagata, 1994, 1996). The labeled cells were found in all zones of the adrenal cortex, i. e. the zona glomerulosa, fasciculata, reticularis of the cortex (Fig. 11A) as well as the medulla (Fig. 11B) from immature prenatal stage to mature postnatal senescent ages. The labeling indices in respective zones showed the maximum at perinatal stage and then gradually decreased to senescent stages. On EMRAG the cell organelles in the labeled cells (Fig. 11C) were less developed than the unlabeled cells in the same zone at the same aging stage (Ito and Nagata, 1996).

Among various hormones available for radioautography, we studied the intracellular localization of ^{3}H-methyl predonisolone which is a synthetic adrenocortical steroid (Nagata et al., 1978b). Mouse adrenals and liver tissue blocks were labeled in vitro with ^{3}H-methyl predonisolone (Daiichi Pure Chemical, Tokyo, Japan, 24.7 GBq/mM, 3.7 kBq/ml) resolved in Eagle's MEM supplemented with 10% bovine serum for 1 hr. Tissues were quickly frozen in cooled isopentane at -165 °C, freeze-dried and embedded in Epon, or cryosectioned and freeze-dried, dry-mounted with Konica NR-H2 emulsion, exposed for 60 days, and developed. With EMRAG, freeze-dried, Epon embedded sections showed silver grains on the nucleus, nucleolus, endoplasmic reticulum, mitochondria, Golgi apparatus and cytoplasmic matrix or both adrenal and liver cells of mice. Wet-mounting radioautograms showed fewer grains on the nucleus and cytoplasm. From the results, it is concluded that the soluble ^{3}H-methyl predonisolone is distributed diffusely in the cell body, while the insoluble compounds are incorporated in the chromatin, nucleolus, nuclear envelopes, endoplasmic reticulum and mitochondria (Nagata et al., 1978b).

6.8. The nervous system

6.8.1. The brains

DNA synthesis was studied in the cerebella of 9 groups of aging mice from embryo to postnatal year 1. The labeled nuclei, both the precursors of neurons and glioblasts, were observed in the external granular layer of the cerebella by LMRAG (Fig. 12A) and EMRAG (Fig. 12B) from embryonic day 19 to postnatal day 14 and disappeared in 1 month. The peak of labeling index was at postnatal day 3. The endothelial cells of the cerebellar vessels were progressively labeled, reaching the peak at 1 week after birth (Cui, 1995).

Changes of glucose uptake in the gerbil hippocampus were also studied using ^{3}H-deoxyglucose by cryo-

fixation, freeze-substitution and dry-mounting radioautography under post-ischemic conditions. The results demonstrated that the neurons subjected to ischemia revealed higher uptake of soluble glucose (Imaizumi et al., 1987).

6.9. Sensory organs

6.9.1. The eye

Nucleic acid synthesis of both DNA and RNA was first studied in the ocular tissues of chick embryos from day 1 to day 14 by light and electron microscopic radioautography (Gunarso, 1984a,b). It was shown that the cells labeled with ^{3}H-thymidine were most frequently observed in the posterior region of the day 2 chick embryo optic vesicle (Fig. 13A) and the labeled cells moved from anterior to posterior regions, decreasing from day 3 to day 7. On the other hand, the number of silver grains incorporating ^{3}H-uridine increased from day 1 to day 7 (Fig. 13B) and was greater in the anterior region than in the posterior region (Gunarso et al., 1996). Then, DNA and RNA syntheses in the ocular tissues of aging mice were also studied. The ocular tissues

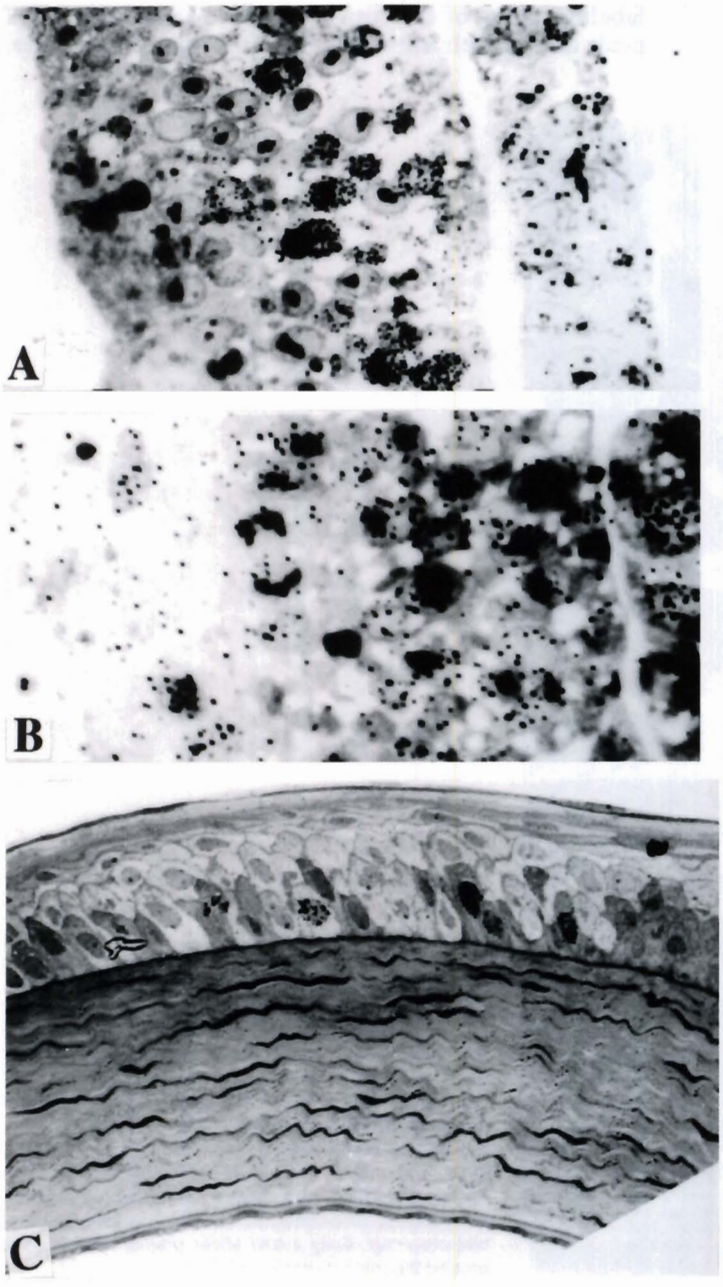

Fig. 13. LMRAG of the ocular tissues of chickens and mice, demonstrating macromolecular synthesis. **A.** The posterior region of the optic vesicle of an chicken embryo incubated for 2 days, injected with ^{3}H-thymidine demonstrating DNA synthesis 1 hr before fixation. Only several nuclei in the retinal layer at the center of the picute are labeled with silver grains. The inner limiting membrane is at the left and the pigment epithelium at the right. x 1,000. **B.** The posterior region of the optic vesicle of an chicken embryo incubated for 2 days, injected with ^{3}H-urididine demonstrating RNA synthesis 1 hr before fixation. Many silver grains are localized over all the cell nuclei, nucleoli and cell bodies of the retinal cells. The inner limiting membrane is at the left and the pigment epithelium at the right. x 1,000. **C.** The cornea of an aged mouse at 1 year after birth, injected with ^{3}H-thymidine demonstrating DNA synthesis. Silver grains are localized over the several nuclei of the epithelial cells (upper half), but no stromal cells or endothelial cells are labeled. x 1,200

obtained from groups of ddY mice litter at ages varying from fetal day 9, 12, 14, 16, 19 to postnatal day 1, 3, 7, 14 were labeled with ^{3}H-thymidine in vitro and radioautographed (Kong et al., 1992b; Kong, 1993). The labeling indices of retina and pigment epithelium were higher in earlier stages than in later stages, during which they steadily declined. However, the retina and pigment epithelium followed different courses in their changes of labeling indices during embryonic development. In the retina, the labeling indices in the vitreal portions were more than those in the scleral portions during the earlier stages. However, the indices of scleral portions were more than those in the vitreal portions in the later stages. Comparing the three regions of the retina of mouse: anterior, equatorial and posterior, the labeling indices of the anterior regions were generally higher than those of the equatorial and posterior regions. In the pigment epithelium, the labeling indices gradually increased in the anterior region, but decreased in the equatorial and the posterior regions through all developmental stages. These results suggest that the proliferation of both the retina and pigment epithelium in the central region occurred earlier than those of the peripheral regions (Kong et al., 1992b; Kong, 1993). In the juvenile and adult stages, however, the labeled cells were localized at the middle of the bipolar-photoreceptor layer of the retina, where was supposed to be the undifferentiated zone (Gao et al., 1992a, b). In the corneas of aging mice, the labeled cells were localized in the epithelial cells at prenatal day 19 to postnatal year 1 (Fig. 13C). The labeling index of the corneal epithelial cells reached a peak at 1 month after birth and decreased to 1 year,

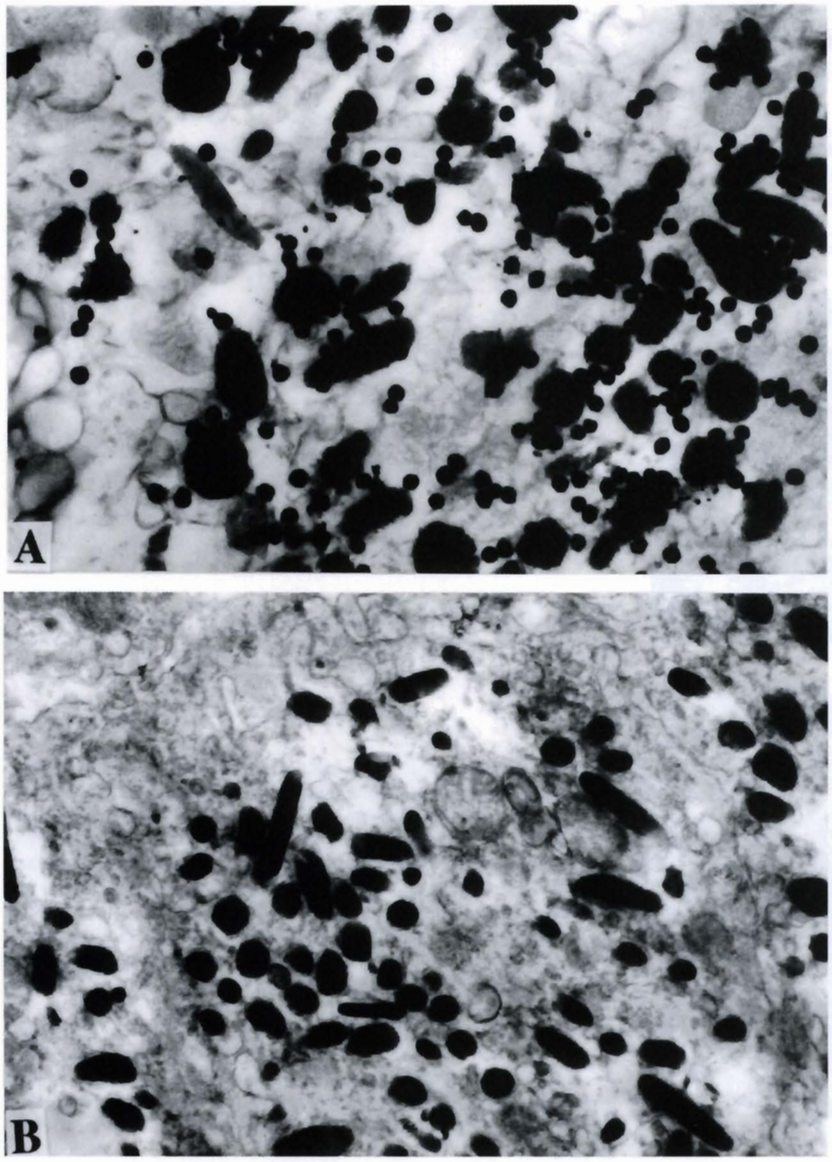

Fig. 14. EMRAG of the ciliary body of a chicken eye, labeled with ^{3}H-befunolol, a beta-blocking agent, showing soluble compounds. **A.** Dry-mounting radioautogram of a melanocyte of the ciliary body, cryofixed in iso-pentane cooled with liquid nitrogen, freeze-dried, embedded in Epon, dry sectioned and dry-mounted. Many silver grains can be seen over the melanosomes, demonstrating soluble compounds. x 8,000. **B.** Wet-mounting radioautogram of a melanocyte of the same tissue as in Fig. 14A, but fixed chemically with glutaraldehyde and osmium tetroxide, dehydrated, embedded in Epon, wet-sectioned and wet-mounted. Only a few silver grains can be seen around the melanosomes. x 6,000

while the indices of stromal and endothelial cells reached a peak at 3 days after birth and disappeared completely from postnatal 1 month to year 1 (Gao et al. 1993). On the other hand, when the ocular tissues were labeled with ^{3}H-uridine, silver grains appeared over all cell types at all stages of development and aging. The grain counts in the retina and the pigment epithelium increased from prenatal day 9 to postnatal day 1 in the retinal cells, while they increased from prenatal day 12 to postnatal day 7 in the pigment epithelial cells (Kong et al., 1992a).

The protein synthesis of the retina in aging mouse as revealed by ^{3}H-leucine incorporation demonstrated that the number of silver grains in bipolar cells and photoreceptor cells was most intense at embryonic stage and early postnatal days. The peak was 1 day after birth and decreased from 14 days to 1 year after birth. (Toriyama, 1995).

On the other hand, glycoprotein synthesis demonstrated by ^{3}H-glucosamine radioautography showed changes of incorporation in the cornea. Silver grains were located in the epithelial cells, the stromal fibroblasts and the endothelial cells from prenatal day 19 to postnatal month 6. No silver grains were observed in the lamina limitans anterior (Bowman's membrane) or the lamina limitans posterior (Descemet's membrane). The grain densities were more observed in the endothelial cells of prenatal day 19 animals, but more in the epithelial cells of postnatal day 1, 3, and 1 week animals. From the results, it was shown that the glycoprotein synthetic activity in respective cell types in the cornea of mouse changed with aging of the animals (Nagata et al., 1995).

Distributions of some of the ophthalmological drugs used for the treatment of glaucoma patients were examined in the ocular tissues. Bupranolol is a beta-blocking agent widely used as an eye drop for glaucoma in the USA and Japan. ^{14}C-bupranolol was experimentally instilled into the eyes of white rabbits and the ocular tissues were enucleated after 15 and 30 minutes, cryo-fixed in liquid nitrogen and the frozen tissues were cryo-sectioned and either freeze-dried or thaw-mounted onto glass slides, followed by either dry-mounting or wet-mounting radioautography. The results showed that silver grains by dry-mounting RAG appeared intensely in the conjunctival and corneal epithelia at 15 minutes, then they decreased there and increased in the ciliary bodies at 30 minutes. These results demonstrated that this drug penetrated the conjunctiva and cornea and accumulated in the ciliary bodies (Tsukahara et al., 1980).

Befunolol is a beta-blocking agent synthesized by Kaken Co., Ltd. Tokyo, Japan. Its chemical structure is 2-acethyl-7(2-hydroxy-3-isopropylamino-propoxy) benzofuran hydrochloride, which was labeled with ^{3}H by New England Nuclear Co., Boston, MA, USA (Yamabayashi et al., 1981; Nagata and Yamabayashi, 1983). The ocular tissues of chickens were taken out, cut into small pieces and labeled with ^{3}H-befunolol in Eagle's MEM (3.7 MBq/ml) in a CO_2 incubator for 30 to 60 minutes. The tissues were cryo-fixed in liquid nitrogen and some of them were dry-sectioned, and some were freeze-dried or freeze-substituted and embedded in Epon, dry-sectioned and dry-mounted. Dry-mounting radioautograms revealed that many silver grains were found over the melanosomes of the pigmented cells demonstrating soluble compounds (Fig. 14A). On the contrary, only few silver grains were found over the melonosomes of the pigmented cells of the iris and the ciliary bodies by wet-mounting radioautography (Fig. 10B). From the results, it was found that soluble ^{3}H-befunolol was accumulated specifically over the melanosomes of the pigmented cells (Nagata and Yamabayashi, 1983).

6.9.2. The skin

When 8 groups of salamander larvae at 4, 6, 8 weeks and 12 months after hatching were injected with ^{3}H-thymidine and the skins from both the forelimbs and hindlimbs were taken out and radioautographed, the labeling indices of epidermal cells increased from 4 weeks to 6 week showing peaks and decreased from 8 weeks and reached 0 at 8 months. These results demonstrated the aging changes of DNA synthesis in the skin (Kobayashi et al., 1994).

7. Concluding remarks

The methods we have developed in our laboratory to demonstrate both soluble and insoluble radioactive compounds by either wet-mounting or dry-mounting procedures and to quantitate macromolecular synthesis or small molecular compounds, preparing many radioautograms at once, have been described in detail.

The results from these methods applied to macromolecular syntheses, DNA, RNA, proteins, glucides and lipids in various organs, as well as the results from dry-mounting procedure, demonstrating hormones, inorganic substances, drugs in various organ systems have been briefly summarized.

The results obtained from these methods include not only 3-dimensional structures of the organs but also the 4-dimensional features taking the time dimension into account by labeling cells and localizing the sites of incorporation, synthesis and discharge of the labeled compounds in connection with the time lapse and aging of animals. The technologies which have been developed recently and the results obtained from their applications to various organs should be systematized as a new field of science designated as radioautographology in contrast to the mere techniques which should be designated as radioautography.

The methodologies are now well developed and completed and should be applicable to any substances and animal organs or tissues and cells for analyzing the cellular functions in situ at cell organelle and molecular levels. These technologies should be designated as

general radioautographology. On the other hand, the results obtained from the applications of radioautography to biology using various kinds of labeled compounds can be classified into several fields, i.e. anatomy, histology, embryology, pathology, pharmacology cellular biology and molecular biology. The results obtained from such applications should be systematized as a new field of science designated as special radioautographology. The present author advocates a new concept of "radioautographology" (Nagata, 1996b). Now the new science, named as radioautographology, consisting of both subdivisions, general radioautographology (technology) and special radioautographology (applications), is expected to develop rapidly in various fields of biological sciences.

References

Altmann R. (1890). Die Elementarorganismen und ihre Beziehungen zur Zellen. Veit u. Co., Leipzig.

Appleton T.C. (1964). Autoradiography of soluble labeled compounds. J. Roy. Microsc. Soc. 83, 277-281.

Bernhard W. and Leduc E.H. (1967). Ultrathin frozen sections. I. Methods and ultrastructural preservation. J. Cell Biol. 34, 757-771.

Chen S., Gao F., Kotani A. and Nagata T. (1995). Age-related changes of male mouse submandibular gland: A morphometric and radioautographic study. Cell. Mol. Biol. 41, 117-124.

Christensen A.K. (1971). Frozen thin sections of fresh tissue for electron microscopy, with a description of pancreas and liver. J. Cell Biol. 51. 772-804.

Cui H. (1995). Light microscopic radioautographic study on DNA synthesis of nerve cells in the cerebella of aging mice. Cell. Mol. Biol. 41, 1139-1154.

Duan H., Gao F., Li S. Hayashi K. and Nagata T. (1992). Aging changes of the fine structure and DNA synthesis of esophageal epithelium in neonatal, adult and old mice. J. Clin. Eletron Microsc. 25, 452-453.

Duan H., Gao F., Li S. and Nagata T. (1993). Postnatal development and aging of esophageial epithelium in mouse: a light and electron microscopic radioautographic study. Cell. Mol. Biol. 39, 309-316.

Duan H., Gao F., Oguchi K and NagataT. (1994). Light and electron microscopic radioautographic study on the incorporation of ^{3}H-thymidine into the lung by means of a new nebulizer. Arznemittel-Forsch. 44, 880-883.

Edwards L.C. and Udupa K.N. (1957). Autoradiographic determination of S^{35} in tissues after injection of methionin-S^{35} and sodium sulfate-S^{35} J. Biophys. Biochem. Cytol. 3, 757-770.

Fitzgerald P.J. (1961). Dry-mounting autoradiographic technic for intracellular localization of water-soluble compounds in tissue sections. Lab. Invest. 10, 846-856.

Fujii Y., Ohno S., Yamabayashi S., Usuda N., Saito H., Furuta S. and Nagata T. (1980). Electron microscopic radioautography of DNA synthesis in primary cultured cells from an IgG myeloma patient. J. Clin. Electron Microsc. 13, 582-583.

Futaesaku Y. and Mizuhira V. (1986). Negative-staining autoradiography: A new technique for ultracryotomy utilizing an interposed film. J. Histochem. Cytochem. 34, 1085-1094.

Gao F. (1993). Study on the macromolecular synthesis in aging mouse seminiferous tubules by light and electron microscopic radioautography. Cell. Mol. Biol. 39, 659-672.

Gao F., Li, S., Duan H., Ma H. and Nagata T. (1992a). Electron microscopic radioautography on the DNA synthesis of prenatal and postnatal mice retina after labeled thymidine injection. J. Clin. Electron Microsc. 25, 721-722.

Gao F., Toriyama K. and Nagata T. (1992b). Light microscopic radioautographic study on the DNA synthesis of prenatal and postnatal aging mouse retina after labeled thymidine injection. Cell. Mol. Biol. 38, 661-668.

Gao F., Toriyama K., Ma H. and Nagata T. (1993). Light microscopic radioautographic study on DNA synthesis in aging mice cornea. Cell. Mol. Biol. 39, 435-441.

Gao F., Ma H., Sun L. and Nagata T. (1994), Electron microscopic radioautographic study on the nucleic acid and protein synthesis in the aging mouse testis. Med. Electron Microsc. 27, 360-362.

Gao F., Chen S., Sun L., Kang W., Wang Z. and Nagata T. (1995a). Radioautographic study of the macromolecular synthesis of Leydig cells in aging mice testis. Cell. Mol. Biol. 41, 145-150.

Gao F., Jin C., Ma H., Sun, L. and Nagata T. (1995b). Ultrastructural and radioautographic studies on DNA synthesis in Leydig cells of aging mouse testis. Cell. Mol. Biol. 41, 151-160.

Gersh I. (1932). The Altmann technique for fixation by drying while freezing. Anat. Rec. 53, 309-324.

Gersh I. (1956). The preparation of frozen-dried tissue for electron microscopy. J. Biophys. Biochem. Cytol. Suppl. 2, 37-55.

Gunarso W. (1984a). Radioautographic studies on the nucleic acid synthesis of the retina of chick embryo. I. Light microscopic radioautography. Shinshu Med. J. 32, 231-240.

Gunarso W. (1984b). Radioautographic studies on the nucleic acid synthesis of the retina of chick embryo. I. Electron microscopic radioautography. Shinshu Med. J. 32, 241-248.

Gunarso W., Gao F., Cui, H., Ma H. and Nagata T. (1996). A light and electron microscopic radioautographic study on RNA synthesis in the retina of chick embryo. Acta Histochem. 98, 309-322.

Hammarstrom L., Appelgren L-E. and Ullberg S. (1965). Improved method for light microscopy autoradiography with isotopes in water-soluble form. Exp. Cell Res. 37, 608-613.

Hanai T. (1993), Light microscopic radioautographic study of DNA synthesis in the kidneys of aging mice. Cell. Mol. Biol. 39, 81-91.

Hanai T. and Nagata T. (1994a). Study on the nucleic acid synthesis in the aging mouse kidney by light and electron microscopic radioautography. In: Radioautography in medicine. Nagata T. (ed). Shinshu University Press. Matsumoto. pp 209-214,

Hanai T. and Nagata T. (1994b). Electron microscopic study on nucleic acid synthesis in perinatal mouse kidney tissue. Med. Electron Microsc. 27, 355-357.

Hanai T., Usuda N., Morita T., Shimizu T. and Nagata T. (1993). Proliferative activity in the kidneys of aging mice evaluated by PCNA/cyclin immunohistochemistry. Cell. Mol. Biol. 39, 181-191.

Hayashi K. and Nagata T. (1993). Radioautographic study on ^{3}H-thymidine incorporation at different stages of muscle development in aging mice. Cell. Mol. Biol. 39, 553-560.

Imaizumi K., Kogure K., Kataoka S. and Nagata T. (1987), Quantitative analysis of glucose after transient ischemia in the gerbil hippocampus by light and electron microscope radioautography. Brain Res. 416, 175-179.

Ito M. (1995). The radioautographic studies on aging change of DNA synthesis and the ultrastructural development of mouse adrenal gland. Cell. Mol. Biol. 42, 14-29.

Ito M. and Nagata T. (1994). Radioautographic study on DNA synthesis

in adrenal glands of developing and aging mice. J. Histochem. Cytochem. 42, 988.

Ito M. and Nagata T. (1996). Electron microscopic radioautographic studies on DNA synthesis and ultrastructure of aging mouse adrenal gland. Med. Electron Microsc. 29, (in press).

Jamieson J.D. and Palade G.E. (1967). Intracellular transport of secretory proteins in the pancreatic exocrine cells. J. Cell Biol. 34, 577-615.

Jin C. (1995). Study on DNA synthesis of aging mouse colon by light and electron microscopic radioautography. Cell. Mol. Biol. 41, 255-268.

Jin C. and Nagata T. (1995a). Light microscopic radioautographic study on DNA synthesis in cecal epithelial cells of aging mice. J. Histochem. Cytochem. 43, 1223-1228.

Jin C. and Nagata T. (1995b). Electron microscopic radioautographic study on DNA synthesis in cecal epithelial cells of aging mice. Med. Electron Microsc. 28, 71-75.

Joukura K. and Nagata T. (1995). Aging changes of ^{3}H-glucosamine incorporation into mouse kidney observed by radioautography. Acta Histochem. Cytochem. 28, 494-494.

Kinter W.B., Leape L.L. and Cohen J.J. (1960). Autoradiographic study of Diodrast-I^{131} transport in Necturus kidney. Am. J. Physiol. 199, 931-942.

Kobayashi K. and Nagata T. (1994). Light microscopic radioautographic studies on DNA, RNA and protein synthesis in human synovial membrane of rheumatoid arthritis patients. J. Histochem. Cytochem. 42, 982-982.

Kobayashi K., Matsumura K. and Nagata T. (1995). Aging changes of DNA synthesis in salamander cartilage and skin by microscopic radioautography. Acta Anat. Nippon. 70, B20-20.

Komiyama K., Iida F., Furihara R., Murata F. and Nagata T. (1978). Electron microscopic radioautographic study on ^{125}I-albumin in rat gastric mucosal epithelia. J. Clin. Electron Microsc. 11, 428-429.

Kong Y. (1993). Electron microscopic radioautographic study on DNA synthesis in perinatal mouse retina. Cell. Mol. Biol. 39, 55-64.

Kong Y., Usuda N., Morita T., Hanai T. and Nagata T. (1992a). Study on RNA synthesis in the retina and retinal pigment epithelium of mice by light microscopic radioautography. Cell. Mol. Biol. 38, 669-678.

Kong Y., Usuda N. and Nagata T. (1992b). Radioautographic study on DNA synthesis of the retina and retinal pigment epithelium of developing mouse embryo. Cell. Mol. Biol. 38, 263-272.

Leblond C.P. (1981). The life history of cells in renewing systems. Am. J. Anat. 160, 113-158.

Li S. (1994). Relationship between cellular DNA synthesis, PCNA expression and sex steroid hormone receptor status in the developing mouse ovary, uterus and oviduct. Histochemistry 102, 405-413.

Li S. and Nagata T. (1995). Nucleic acid synthesis in the developing mouse ovary, uterus and oviduct studied by light and electron microscopic radioautography. Cell. Mol. Biol. 41, 185-195.

Li S., Gao F., Duan H. and Nagata T. (1992). Radioautoagraphic study on the uptake of $^{35}SO_4$ in mouse ovary during the estrus cycle. J. Clin. Electron Microsc. 25, 709-710.

Lison L. (1960) Histochimie et Cytochimie Animales. 3rd ed. Gauthier-Villards. Paris. 532pp.

Luft J.E. (1961). Improvements in epoxy resin embedding methods. J. Biophys. Biochem. Cytol. 9, 409-414.

Ma H. (1988). Studies on DNA synthesis of aging mice by means of light microscopic radioautography. Acta Anat. Nippon. 61, 37-147.

Ma H. and Nagata T. (1988). Studies on DNA synthesis of aging mice by means of electron microscopic radioautography. J. Clin. Electron Microsc. 21, 715-716.

Ma H. and Nagata T. (1990a). Electron microscopic radioautographic studies on DNA synthesis in the hepatocytes of aging mice as observed by image analysis. Cell. Mol. Biol. 36, 73-84.

Ma H. and Nagata T. (1990b). Study on RNA synthesis in the livers of aging mice by means of electron microscopic radioautography. Cell. Mol. Biol. 36, 589-600 .

Ma H. and Nagata T. (1991). Protein synthesis in the livers of aging mice studied by electron microscopic radioautography. Cell. Mol. Biol. 37, 607-615 .

Ma H., Gao F., Olea M.T. and Nagata T. (1992). Protein synthesis in the livers of aging mice studied by electron microscopic radioautography. J. Clin. Electr. Microsc. 25, 536-537.

Matsumura H., Kobayashi Y., Kobayashi K. and Nagata T. (1994). Light microscopic radioautographic study of DNA synthesis in the lung of aging salamander, *Hynobius nebulosus*. J. Histochem. Cytochem. 42, 1004-1004.

Miller O.L. Jr., Stone G.E. and Prescott D.M. (1964). Autoradiography of soluble materials. J. Cell Biol. 23, 654-658.

Mizuhira V., Shiihashi M. and Futaesaku Y. (1981). High-speed electron microscope autoradiographic studies of diffusible compounds. J. Histochem. Cytochem. 29, 143-160.

Mizuhira V., Uchida K., Totsu J. and Shindo H. (1968). Studies on the absorption of S-benzoylthiamine O-monophosphate (in Japanese). Vitamins (Japanese) 38, 334-346.

Momose Y. and Nagata T. (1993). Radioautoagraphic study on the intracellular localization of a hypolipidemic agent, bezafiabrate, a peroxisome proliferator, in cultured rat hepatocytes. Cell. Mol. Biol. 39, 773-781.

Momose Y., Naito J. and Nagata T. (1989). Radioautoagraphic study on the localization of an anti-allergic agent, tranilast, in the rat liver. Cell. Mol. Biol. 35, 347-355.

Momose Y., Naito J., Suzawa H., Knazawa M. and Nagata T. (1995). Radioautographic study on the intracellular localization of bezafibrate in cultured rat hepatoctyes. Acta Histochem. Cytochem. 28, 61-66.

Morita T. (1993). Radioautographic study on the aging change of ^{3}H-glucosamine uptake in mouse ileum. Cell. Mol. Biol. 39, 875-884.

Morita T., Usuda N., Hanai T. and Nagata T. (1993). Changes of colon epithelium proliferation due to individual aging with PCNA/cyclin immunostaining comparing with ^{3}H-thymidine radioautography. Histochemistry 101, 13-20.

Murata F., Momose Y., Yoshida K. and Nagata T. (1977). Incorporation of ^{3}H-thymidine into nuclei of mast cells in adult rat peritoneum. Shinshu Med. J. 25, 72-77.

Murata F., Yoshida K., Ohno S. and Nagata T. (1978). Ultrastructural and electron microscopic radioautographic study on the mastocytoma cells and mast cells. J. Clin. Electron Microsc. 13, 582-583.

Murata F., Yoshida K., Ohno S. and Nagata T. (1979). Electron microscopic radioautography using a combination of phenidone developer and domestic emulsion. Acta Histochem. Cytochem. 12, 443-450.

Nagata T. (1967). On the increase of binucleate cells in the ganglion cells of dog small intestine due to experimental ischemia. Med. J. Shinshu Univ. 12, 93-113.

Nagata T. (1972). Electron microscopic dry-mounting autoradiography. Proc. 4th Internat. Cong. Histochem. Cytochem. 43-44.

Nagata T. (1982). Simple method for mass production of radioautographs. The Cell (Saibo, in Japanese). 14, 40-50.

Nagata T. (1991). Electron microscopic radioautography and analytical electron microscopy. J. Clin. Electron Microsc. 24, 441-442.

Nagata T. (1992) Radiolabeling of soluble and insoluble compounds as demonstrated by light and electron microscopy. In: Recent advances in cellular and molecular biology. Vol. 6. Molecular biology of pyridines and DNA, peroxisomes, organelles and cell movements. Wegmann R.J. and Wegmann M.A. (eds). Peeters Press. Leuven. Belgium. pp 9-21.

Nagata T. (1993a) Quantitative analysis of histochemical reactions, Image analysis of light and electron microscopic radioautograms. Acta Histochem. Cytochem. 26, 281-191.

Nagata T. (1993b). Quantitative light and electron microscopic radioautographic studies on macromolecular synthesis in several organs of prenatal and postnatal aging mice. Chinese J. Histochem. Cytochem. 2, 106-108.

Nagata T. (1994a). Electron microscopic radioautography with cryofixation and dry-mounting procedure. Acta Histochem. Cytochem. 27, 471-489.

Nagata T. (1994b). Radioautography in Medicine, Shinshu University Press. Matsumoto. 268 pp.

Nagata T. (1994c). Application of electron microscopic radioautography to clinical electron microscopy. Med. Electron Microsc. 27, 191-212.

Nagata T. (1995a). Light and electron microscopic radioautographic studies on macromolecular synthesis in digestive organs of aging mice. Cell. Mol. Biol. 41, 21-38.

Nagata T. (1995b). Three-dimensional observation of whole mount cultured cells stained with histochemical reactions by ultrahigh voltage electron microscopy. Cell. Mol. Biol. 41, 783-792.

Nagata T. (1995c). Morphometry in anatomy, image analysis on fine structure and histochemical reactions with special reference to radioautography. Ital. J. Anat. 100 (Suppl. 1). 591-605.

Nagata T. (1995d). Histochemistry of the organs. Application of histochemistry to anatomy. Acta Anat. Nippon. 70, 448-471.

Nagata T. (1996a). Techniques and application of electron microscopic radioautography. J. Electron Microsc. 45, 258-274.

Nagata T. (1996b). Radioautographology, general and special. Cell. Mol. Biol. 42, S11-12.

Nagata T. and Murata F. (1977). Electron microscopic dry-mounting radioautography for diffusible compounds by means of ultracryotomy. Histochemistry 54, 75-82.

Nagata T. and Nawa T. (1966). A modification of dry-mounting technique for radioautography of water-soluble compounds. Histochemie 7, 370-371.

Nagata T. and Shimamura K. (1958). Radioautographic studies on calcium absorption. I. Calcium absorption in the stomach of rat. Med. J. Shinshu Univ. 3, 83-90.

Nagata T. and Shimamura K. (1959a). Radioautographic studies on calcium absorption. II. Calcium absorption in the intestines of rat. Med. J. Shinshu Univ. 4, 1-10.

Nagata T. and Shimamura K. (1959b). Radioautographic studies on calcium absorption. III. Distribution of radiocalcium in the liver and the kidney of rat after oral administration. Med. J. Shinshu Univ. 4, 11-18.

Nagata T. and Usuda N. (1986). Studies on the nucleic acid synthesis in pancreatic acinar cells of aging mice by means of electron microscopic radioautography. J. Clin. Electron Microsc. 19, 486-487.

Nagata T. and Usuda N. (1993). Electron microscopic radioautography of protein in pancreatic acinar cells of aging mice. Acta Histochem. Cytochem. Microsc. 26, 481-481.

Nagata T. and Yamabayashi S. (1983). Intracellular localization of ^{3}H-befunolol by means of electron microscopic radioautography of cryofixed ultrathin sections. J. Clin. Electron Microsc. 16, 737-738.

Nagata T., Shibata O. and Omochi S. (1961). A new method for radioautographic observation on isolated cells. Histochemie 2, 255-259.

Nagata T., Shibata S. and Nawa T. (1967a). Simplified methods for mass production of radioautographs. Acta Anat. Nippon. 42, 162-166.

Nagata T., Shibata S. and Nawa T. (1967b). Incorporation of tritiated thymidine into mitochondrial DNA of the liver and kidney cells of chickens and mice in tissue culture. Histochemie 10, 305-308.

Nagata T., Nawa T. and Yokota S. (1969). A new technique for electron microscopic dry-mounting radioautography of soluble compounds. Histochemie 18, 241-249.

Nagata T., Ohno S. and Murata F. (1977a). Electron microscopic dry-mounting radioautography for soluble compounds. Acta Phamacol. Toxicol. 41, 62-63.

Nagata T., Murata F., Yoshida K., Ohno S. and Iwadare N. (1977b). Whole mount radioautography of cultured cells as observed by high voltage electron microscopy. Proc. 5th Internat. Cong. High Voltage Electron Microsc. 347-350

Nagata T., Yoshida K. and Murata F. (1977c). Demonstration of hot and cold mercury in the human thyroid tissues by means of radioautography and chemography. Acta Pharmacol. Toxicol. 41, 60-61.

Nagata T., Ohno S, Yoshida K. and Murata F. (1978a). A simple picking up device for cryosections. Science Tools 25, 59-60.

Nagata T., Yoshida K., Ohno S. and Murata F. (1978b). Ultrastructural localization of soluble and insoluble ^{3}H-methyl prednisolone as revealed by electron microscopic dry-mounting radioautography. Proc. 9th Internat. Congr. Electron Microsc. 2, 40-41.

Nagata T., Ohno S., Yamabayashi S., Fujii S. and Kawahara I. (1980). Radioautographic studies on macromolecular synthesis of various tissues of mice by aging. Acta Anat. Nippon. 55, 77.

Nagata T., Ohno S., Yoshida K. and Murata F. (1982). Nucleic acid synthesis in proliferating peroxisomes of rat liver as revealed by electron microscopical radioautography. Histochem. J. 14, 197-204.

Nagata T., Usuda N. and Ma H. (1984). Electron microscopic radioautography of nucleic acid synthesis in pancreatic acinar cells of prenatal and postnatal aging mice. Proc. XIth Intern. Cong. Electr. Microsc. 3, 2281-2282.

Nagata T., Nishigaki T. and Momose Y. (1986). Localization of antiallergic agent in rat mast cells demonstrated by light and electron microscopic radioautography. Acta Histochem. Cytochem. 19, 669-683.

Nagata T., Kawahara I., Usuda N., Maruyama M. and Ma H. (1988a). Radioautographic studies on the glycoconjugate synthesis in the gastrointestinal mucosa of the mouse. In: Glycoconjugate in medicine. Ohyama M. and Muramatsu T. (eds). Profes. Postgrad. Service. Tokyo. pp 251-256.

Nagata T., Usuda N., Maruyama M. and Ma H. (1988b). Electron microscopic radioautographic study on lipid synthesis in perinatal mouse pancreas. J. Clin. Electr. Microsc. 21, 756-757.

Nagata T., Usuda N. and Ma H. (1990). Electron microscopic radioautography of lipid synthesis in pancreatic cells of aging mice. J. Clin. Electr. Microsc. 23, 841-842.

Nagata T., Usuda N., Suzawa H. and Kanzawa M. (1992). Incorporation of ^{3}H-glucosamine into the pancreatic cells of aging mice as demonstrated by electron microscopic radioautography. J. Clin. Electr. Microsc. 25, 646-647.

Nagata T., Cui H. and Gao F. (1995). Radioautographic study on glycoprotein synthesis in the ocular tissues. J. Kaken Eye Res. 14, 11-18.

Nishigaki T., Momose Y. and Nagata T. (1987). Light microscopic radioautographic study of the localization of anti-allergic agent, Tranilast, in rat mast cells. Histochem. J.19, 533-536.

Nishigaki T., Momose Y. and Nagata T. (1990). Localization of the anti-allergic agent tranilast in the urinary bladder of rat as demonstrated by light microscopic radioautography. Arzneimittel-Forsch. 40, 272-275.

Oguchi K. and Nagata T. (1981). Electron microscopic radioautographic observation on activated satellite cells in dystrophy chickens. In: Clinical studies on the etiology of muscular dystrophy. Annual Report on Neurological Diseases 1981. The Ministry of Welfare of Japan, ed. Tokyo. pp. 30-33.

Olea M.T. and Nagata T. (1992a). Simultaneous localization of ^{3}H-thymidine incorporation and acid phosphatase activity in mouse spleen. Electron microscopic radioautography and cytochemistry. Cell. Mol. Biol. 38,115-122.

Olea M.T. and Nagata T. (1992b). A radioautographic study on RNA synthesis in aging mouse spleen after ^{3}H-uridine labeling in vitro. Cell. Mol. Biol. 38, 399-405.

Oliveira S.F., Abrahamsohn P.A., Nagata T. and Zorn T.M.T. (1995). Incorporation of ^{3}H-amino acids by endometrial stromal cells during decidualization in the mouse. A radioautographical study. Cell. Mol. Biol. 41, 107-116.

Oliveria S.F., Nagata T., Abrahamsohn P.A. and Zorn T.M.T. (1991). Electron microscopic radioautographic study on the incorporation of ^{3}H-proline by mouse decidual cells. Cell. Mol. Biol. 37, 315-323.

Pearse A.G.E. (1968) Histochemistry, theoretical and applied. 3rd. ed. Vol. I. J.&A. Churchill Ltd. London. pp 50-51.

Reynolds E.S. (1963). The use of lead citrate at high pH as an electron opaque stain in electron microscopy. J. Cell Biol. 17, 208-212.

Rogers A.W. Thomas G.H. and Yates K.M. (1965). Autoradiographic studies on the distribution of labeled progesterone in the uterus of the rat. Exp. Cell Res. 40, 668-673.

Sakai T., Shimakura S. and Sakamoto H. (1974). The ultrathin section for low temperature. Proc. 8th Internat. Cong. Electron Microsc. 2, 56-57.

Sakai Y., Ikado S. and Nagata T. (1977). Electron microscopic radioautography of satellite cells in regenerating muscles. J. Clin. Electron Microsc. 10, 508-509.

Sato A. (1978). Quantitative electron microscopic studies on the kinetics of secretory granules in G-cells. Cell Tissue Res. 187, 45-59.

Sato A., Iida F. Furihara R. and Nagata T. (1977). Electron microscopic raioautography of rat stomach G-cells by means of ^{3}H-amino acids. J. Clin. Electron Microsc. 10, 358-359.

Simpson W.L. (1941). An experimental analysis of the Altmann Technic of freezing drying. Anat. Rec. 80, 173-185.

Smitherman T.C., Debons A.F., Pittman J.A. and Stephens V. (1963). Movement of water-soluble material in Mayer's albumin and a simplified dry-mounting method for autoradiography. Nature 198, 499-500.

Stirling C.E. and Kinter W.B. (1967). High resolution radioautography of galactose-^{3}H accumulation in rings of hamster intestine. J. Cell Biol. 35, 585-604.

Stumpf W.E. and Roth L.J. (1964). Vacuum freeze drying of frozen sections for dry-mounting high resolution autoradiography. Stain Technol. 39, 219-223.

Stumpf W.E. and Roth L.J. (1966). High resolution autoradiography with dry-mounting freeze-dried frozen sections. Comparative study of six methods using two diffusible compounds, ^{3}H-estradiol and ^{3}H-mesobilirubinogen. J. Histochem. Cytochem. 14, 274-287.

Stumpf W.E. and Roth L.J. (1969). Autoradiography using dry-mounted freeze-dried sections. In: Autoradiography of diffusible substances. Roth L.J. and Stumpf W.E. (eds). Academic Press. New York and London. pp 69-80.

Sun L. (1995). Age-related changes of RNA synthesis in the lungs of aging mice by light and electron microscopic radioautography. Cell. Mol. Biol. 41, 1061-1072.

Sun L., Gao F., Duan H. and Nagata T. (1994). Light microscopic radioautography of DNA synthesis in pulmonary cells in aging mice. In: Radioautography in medicine. Nagata T. (ed). Shinshu University Press. Matsumoto. pp.201-205.

Sun L., Gao F., Jin C., Duan H. and Nagata T. (1995). An electron microscopic radioautographic study on the DNA synthesis of pulmonary tissue cells in aging mice. Med. Electron Microsc. 28, 129-131.

Sun L., Gao F., Jin C. and Nagata T. (1996). DNA synthesis in the aging mice tracheae by means of light and electron microscopic radio-autography. J. Histochem. Cytochem. (Submitted for publication).

Suzuki K., Imada T., Gao F., Ma H. and Nagata T. (1994). Radioauto-graphic study of benidipine hydrochloride, localization in the mesenteric artery of spontaneously hypertensive rat. Arzneimittel-Forsch. 44, 129-133.

Terauchi A. and Nagata T. (1993). Observation on incorporation of ^{3}H-taurine in mouse skeletal muscle cells by light and electron microscopic radioautography. Cell. Mol. Biol. 39, 397-404.

Terauchi A., Mori T., Kanda H., Tsukada M. and Nagata T. (1988). Radioautographic study of ^{3}H-taurine uptake in mouse skeletal muscle cells. J. Clin. Electron Microsc. 21, 627-628.

Toriyama K. (1995). Study on the aging changes of DNA and protein synthesis of bipolar and photo-receptor cells of mouse retina by light and electron microscopic radioautography. Cell. Mol. Biol. 41, 593-601.

Tsukahara S., Yoshida K. and Nagata T. (1980). A radioautographic study on the incorporation of ^{14}C-bupranolol (beta-blocking agent) into the rabbit eye. Histochemistry 68, 237-244.

Tokuyasu K. (1973). A technique for ultracryotomy of cell suspensions and tissues. J. Cell Biol. 57, 551-565.

Trump B.F. (1969). Autoradiography of diffusible substances. In: Autoradiography of diffusible substances. Roth L.J. and Stumpf W.E. (eds). Academic Press. New York and London. pp 211-240.

Van Harrevelt A. and Crowell J. (1964). Electron microscopy after rapid freezing on a metal surface and substitution fixation. Anat. Rec. 149, 381-386.

Yamabayashi S., Gunarso W., Tsukahara S. and Nagata T. (1981). Incorporation of ^{3}H-befunolol (beta-blocking agent) into melanin granules of ocular tissues in the pigmented rabbits. I. Light microscopic radioautography. Histochemistry 73, 371-375.

Yamada A. (1993). Timely and topologically defined protein synthesis in the peri-implanting mouse endometrium revealed by light and electron microscopic radioautography. Cell. Mol. Biol. 39, 1-12.

Yamada A. and Nagata T. (1992a). Light and electron microscopic

radioautography of DNA synthesis in the endometria of pregnant-ovariectomized mice during activation of implantation window. Cell. Mol. Biol. 38, 763-774.

Yamada A. and Nagata T. (1992b). Light and electron microscopic radioautographic studies of RNA synthesis of periimplanting pregnant mouse uterus during activation of receptivity for blastocyst implantation. Cell. Mol. Biol. 38, 763-774.

Yoshida K., Murata F., Ohno S. and Nagata T. (1978). A modified wire-loop method for quantitative electron microscopic radioautography. Histochemistry 57, 93-96.